Republic of Iraq
Ministry of Higher Education
And Scientific Research
University of Baghdad
College of Education for pure Sciences(Ibn Al-Haitham)

Quantum Mechanics Consideration For Fusion Cross Section

A Thesis
Submitted to the Council of College of Education for pure Sciences
(Ibn Al-Haitham) University of Baghdad
in Partial Fulfillment of the Requirements for
the Degree of Master in
Nuclear Physics

By

Muayad Mohammed Abed

Supervisor

Assist. Prof .Dr.Raad Hameed Majeed

Assist Prof. Dr. Mustafa Kamel Jassim

2014 A.D 1435 H.D

Acknowledgments

In the beginning, praise is to Allah for helping me in everything. I would like to express my deepest gratitude to everyone who has given me the support I needed to complete this thesis .My deep appreciation goes to to Assist Prof. Dr. Raad Hameed Majeed for supervision and thanks to Assist Prof. Dr. Mustafa Kamel Jassim for his help, continuous help and useful discussion during the preparation of this work and Assist Prof. Dr. Hadi Alagealy for his help.

Finally , I would like to thank my dearest people (my parents , brothers , my wife and my children) have been the greatest role in supporting me to accomplish this work with their continuous encouragement and prayers .

Muayad

Supervisor's Certification

We certify that this thesis was prepared under our supervision at University of Baghdad / College of Education Ibn- Al – Haitham / Department of Physics in partial fulfillment of the requirements for the degree of **Master of Science in Physics**.

Signature:

Supervisor: Dr.Raad H .Majeed

Title: Assist Professor
Department of physics
College of Ibn-Al- Haitham
University of Baghdad

Date: / / 2014

Signature:

Supervisor: Dr.Mustafa K. Jassim

Title: Assist Professor
Department of Physics
College of Ibn-Al-Haitham
University of Baghdad

Date: / /2014

In view of the available recommendation, we forward this thesis for debate by the examining committee.

Signature:

Name: Dr.Mohammed Abdul-Nabi Thejeel

Title: (Assist Professor)

"Chairman of Physics Department"

Date: / / 2014

Abbreviations

Symbol	Description	Unit
v	Relative velocity	m/sec
v_1, v_2	Velocities of reacting nuclei	m/sec
$\in$	Center of mass energy	MeV
m_r	Reduced mass of system	Kg
r_n	Nuclear reduce formula	m
Umax	Barrier height for charged particles	MeV
e	Electron charge	c
V	potential	KeV
σ_{12}^{bt}	Beam-target cross section	barn
$\sigma_{12}(\epsilon)$	Center of mass cross section	barn
$< \sigma v >$	reactivity	cm^3/sec
$\sigma(v)$	Cross section	barn
n	Total nuclei number density	Kg/m^3
R12	Reaction rate	cm^3/sec
F1, F2	Atomic fractions	
δ_{ij}	kronecker	
W_r	Imaginary part potential	MeV
$\frac{d\sigma}{d\Omega}$	Differential cross section for nuclear fusion reaction	Srad/barn
F(θ)	Scattering amplitude	
r	distance	m
l	Angular momentum	J.sec
S_l	spin	J.sec
P_l	Barrier penetration factor	
E_{cl}	Critical energy	MeV
$G_\circ$	Green operatore	
$H_\circ$	Hamiltonian	MeV
U	Potential energy	MeV
Z	Atomic number	
A	Mass number	

r_{tp}	Classical turning point	
σ_{geom}	Geometrical cross section	
R	Probability of fuse the nuclei	
$\lambda\!\!\!^{-}$	De-broglie wavelength of system	A° (10^{-10}m)
ħ	Planck constant	J.sec
G	Gamow factor	
α_f	Fine-structure constant	
S(∈)	Astrophysical factor	KeV.barn
σ_l(v)	Resonances the partial cross section	barn
B_l	Function into account nuclear interaction	
T_l	Barrier transmission coefficient	
G_l	Dominant exponential factor	
j	Labels the species	
v_c	Center of mass velocity	m/sec
ξ	Distance factor	cm
$\frac{1}{\theta^2}$	Famous gamow penetration factor	
a	Radius of nuclear well	fermi
F	Central force field	
$b_\circ$	Landan parameter	
Γ	Gamma function	
T	Decay time constant	sec
Γ	Resonance width	MeV
E_r	Resonance energy	MeV
T	Barrier transprancy	
E_l	Laboratory energy	MeV
k	Wave number	m^{-1}
R_e	Real part of potential	KeV
I_m	Imaginary part of potential	KeV

Abbreviations

ITER	International Thermonuclear Experimental Reactor
QCD	Quantum Chromodynamics
EQPET	Electronic Quasi-Particle Expansion
TSC	Tetrahedral Symmetric Condensate
ENDF	Evaluated Nuclear Data File
B-IV	Bench Marking
JET	Joint European Torus
JE	Japan Torus

Abstract

In the current research we have chosen the reactions ($DD, DT, D\,^{3}He$) for nuclear fusion where energies of fusion and temperature of measuring cross section fusion were taken in consideration which have been performed by direct reaction method for complex nucleus, where the treatment was conducted in accordance with models (I, II, III).

A comparison ,also, was conducted to some of related results.

To be noted , all nuclear reactions parameters have been extracted from international references, where they were put in equations to calculate cross section fusion in all fusion reaction channels.

The theoretical calculations were performed by computer simulations of Matlab program version 2009a.

Dedication

To my Father

My Mother

My wife

My Brothers and friends

Muayad

CONTENTS

Chapter one

Introduction

1.1.Controlled Thermonuclear Fusion

Scientists and Engineers studied the release of enormous amounts of energy that occurs when light nuclei fuse together. Their researchs led them first to the successful development of the H-bomb.

Many researchers at the time realized that rather than employing this uncontrolled explosive process to destroy humanity, they could put it to use to serve humankind if only they could find a way to confine the reaction. Thus, the dream of controlled thermonuclear fusion was born.

For example, in 1991 the controlled production of over a megawatt of fusion power (two megajoules of fusion energy were released) was demonstrated in the JET tokamak [**1**], and in 1999 the JT-60U tokamak reported the reproducible production of an equivalent fusion power gain of 1.25 [**2**]; ; that is, more power was released by the fusion reaction than was required to sustain it. As a result of these successes, it is anticipated that the next generation of experimental reactors.[**3**]

In hydrogen fusion two protons have to be brought close enough for the weak nuclear force to convert either of the identical protons into a neutron forming the hydrogen isotope deuterium.Deuterium and tritium are the reactant for the fusion reaction.

1.2 Literature Survey :

Attention and focus on nuclear fusion technology has been started from period of design the hydrogen bomb . So there is a huge number of

researches and articles about this subject. In our research, we focus on articles carried out recently In order to refer to the interest of the developed world in this technology due to the numerous applications of this technology.

- Xing Z. Li in (2002) studied the nuclear fusion data for deuteron-triton resonance near 100 keV are found to be consistent with the selective resonant tunneling model. The feature of this selective resonant tunneling is the selectivity. It selects not only the energy level, but also the damping rate (nuclear reaction rate). When the Coulomb barrier is thin and low, the resonance selects the fast reaction channel; however, when the Coulomb barrier is thick and high, the resonance selects the slow reaction channel. This mechanism might open an approach towards fusion energy with no strong nuclear radiation[**18**].

- Igor D. Kaganovich, Edward A. Startsev, et al in (2003) studied knowledge of ion-atom ionization cross sections is of great importance for many applications. When experimental data and theoretical calculations are not available, approximate formulas are frequently used. Based on experimental data and theoretical predictions, a new fit for ionization cross sections by fully stripped ions is proposed[**19**].

- V. I. Zagrebaev* and V. V. Samarin in (2004) discussed the problem of a quantum-mechanical description of a near-barrier fusion of heavy nuclei that occurs under the conditions of a strong coupling of their relative motion to the rotation of deformed nuclei and to a dynamical deformation of their surfaces is studied. A new efficient method is proposed for numerically solving coupled Schrodinger equations with boundary conditions corresponding to a total absorption of the flux that has overcome a multidimensional Coulomb barrier. The new method involves nolimitations

on the number of channels that are taken into account and makes it possible to calculate cross sections for the fusion of very heavy nuclei that are used in the synthesis of superheavy elements. A global analysis of the relief of the multidimensional potential surface and of the multichannel wave function in the vicinity of the Coulomb barrier provides a clear interpretation of the dynamics of near-barrier nuclear fusion. A comparison with experimental data and with the results produced by the semiempirical model for taking into account the coupling of channels is performed[**20**].

- M. Yu. Romanovsky and W. Ebeling in (2003) discussed the Holtsmark theory is generalized to finite ion clusters. It is shown that large (in comparison to infinite plasmas of the same density) fluctuations of electric microfield in ion clusters appear. The new field distribution shows a longer "tail" than the Holtsmark one. The previously developed semiclassical version of the theory of fusion rates in the presence of plasma electric microfields is applied to the case of nuclear fusion in charged deuterium clusters created by superstrong laser pulses. It is demonstrated that the effect of high free neutron output observed in several experiments with dense deuterium plasma pulses is supported by the action of the electric microfields[**21**].

- Xing Z. Li, Bin l., et al in (2004) discussed the application of selective resonant tunneling model is extended from d + t fusion to other light nucleus fusion reactions, such as d + d fusion and d + 3He. In contrast to traditional formulas, the new formula for the cross-section needs only a few parameters to fit the experimental data in the energy range of interest. The features of the astrophysical S-function are derived in terms of this model. The physics of resonant tunneling is discussed[**22**].

- L.F. Canto, R. Donangelo, et al in (2005) described a semiclassical treatment of nuclear fusion reactions involving weakly bound nuclei. In this treatment, the complete fusion probabilities are approximated by products of two factors: a tunneling probability and the probability that the system is in its ground state at the strong absorption radius. We investigate the validity of the method in a schematic two-channel application, where the channels in the continuum are represented by a single resonant state. Comparisons with full coupled-channels calculations are performed. The agreement between semiclassical and quantal calculations is quite good, suggesting that the procedure may be extended to more sophisticated discretizations of the continuum[**23**].

- L.F. Canto, R. Donangelo, et al in (2005) assessed the validity of the semiclassical approximation of Alder and Winther in the study of breakup and fusion reactions induced by weakly bound projectiles. For this purpose, we are compare semiclassical results with results of full quantum mechanics calculations. We show that the semiclassical method leads to accurate results for the breakup cross section. We then adopt a semiclassical approximation for the l-dependent fusion probabilities and evaluate the cross section
in a schematic two-channel problem. In this case, the semiclassical results are accurate above the Coulomb barrier but cannot reproduce the enhancement of the fusion cross section at sub-barrier energies. We show that this shortcoming can be eliminated through an analytical continuation of the time variable[**24**].

- Ruggero M. Santilli in (2008) proposed apparently for the first time a new type of controlled nuclear fusion called "intermediate" because occurring at energies intermediate between those of the "cold" and "hot" fusions to attempt the resolution of their known insufficiencies. The paper then

presents a progress report on the industrial realizations going on to enhance the net energy output that, currently, is already of the order of five times the used electric energy at relatively low operating power, pressure and temperature, as verifiable in the IBR laboratory in Florida. For this purpose they are showed that known limitations of quantum mechanics, quantum chemistry and special relativity, such as their reversibility in time compared to the irreversibility of all energy re- leasing processes, cause excessive insufficiencies for all controlled nuclear fusions[**25].**

- Mark D., in (2008) spent 17 years perfecting IEC, a fusion process that can potentially allow converting hydrogen and boron directly into electricity producing helium as the only waste product[**26**].

- Xing Z. Li, Qing M. Wei ,et al in (2008) studied the recent ENDF/B VII.0 data are compared with the fitting formula (NRL handbook—Plasma Formulary). The differences between experimental data and the fitting formula for three major fusion cross-sections reveal the need for a replacement to the old 5-parameter fitting formula. The new formula in this paper has only 3 parameters, but its fit with the experimental data is greatly improved because the energy dependence of the incident-channel (deuteron) width is taken explicitly into account through a penetrability function of the Mott form[**27**].

- Yeong E. Kim in (2010) studied theory of Bose-Einstein condensation nuclear fusion (BECNF) has been developed to explain many diverse experimental results of deuteron induced nuclear reactions in metals, observed in electrolysis and gas loading experiments. The theory is based on a single conventional physical concept of Bose-Einstein condensation of deuterons in metal and provides a consistent theoretical description of the experimental results**[28**].

- Bulent Y. , Sakir A. , et al in (2011) discussed a semi-classical method that incorporates the quantum effects of the low-lying vibrational modes
is applied to fusion reactions. The quantum effect is simulated by stochastic sampling of initial zero-point fluctuations of the surface modes. In this model, dissipation of the relative energy into non-collective excitations of
nuclei can be included straightforwardly. The inclusion of dissipation is shown to increase the agreement with the fusion cross section data of Ni isotopes[**29].**

- J.K. Bitok, F.G. Kanyeki, et al in (2012) studied fusion reaction cross-section and angular momentum values help in identifying the possibility of occurrence of a fusion reaction. Fusion cross-sections of heavy ion reactions have been calculated using the semi-classical approach with heavy ions as projectiles. In this model of calculation of fusion reaction cross section, three potentials have been used namely: Coulomb potential, nuclear potential and centrifugal potential. Fusion reactions between the pairs of heavy ions have been studied and their cross-section calculated in semi classical formulation using one-dimensional barrier penetration model, taking scattering potential as the sum of Coulomb, centrifugal and proximity potential[**30]**.

- E.N. Tsyganov, S.B. Dabagov, et al in (2012) discussed accelerator experiment on fusion show a significant increase in the probability when target nuclei are imbedded in a conducting crystal. These experiments open a good perspective on the problem of so-called cold DD nuclear fusion. Here this approach is applied to another fusion processes, and some possible drawbacks are discussed[**31**].

- Rajdeep S., Andreas M. , et al in (2012) studied a general coherent control scheme for speeding up quantum tunneling of proton transfer through Coulombic barriers is analysed. The quantum control scenario is based on

repetitive electron impact ionization pulses that affect the ensuing interference phenomena responsible for quantum dynamics and force the proton to tunnel into classically forbidden regions of configuration space. The scheme is demonstrated for the simplest model of nuclear fusion, hinting at the possible enhancement of reactive scattering based on low energy collisions[**32]**.

- Leo G. Sapogin, Yu. A. Ryabov, in (2013) discussed problems Low Energy Nuclear Reactions with position unitary quantum theory. Probability of these phenomena more than predicts usual quantum theory for small energy[**33**].

- - Igor D. Kaganovich, Ronald C. Davidson, et al in (2013) discussed stripping cross sections in nitrogen have been calculated using the classical trajectory approximation, and the Born approximation of quantum mechanics for the outer shell electrons of 3.2GeV . A large difference in cross section, up to a factor of six, calculated in quantum mechanics and classical mechanics, has been obtained. Because at such high velocities the Born approximation is well validated, the classical trajectory approach fails to correctly predict the stripping cross sections at high energies for electron orbitals with low ionization potential[**34**].

- Falah K. Ahmed, Fouad A. Majeed, et al in (2013) performed Coupled-Channel (CC) calculations to study the effect of coupling to the breakup channel on the calculations of the total reaction cross section σ and the fusion barrier distribution at energies near and below the Coulomb barrier v_b for the systems $^{6}Li + {}^{209}Bi$, $^{7}Li + {}^{209}Bi$ and $^{9}Be + {}^{208}Pb$. The inclusion of breakup reaction enhances the calculations of the total reaction cross section in comparison with the recent available experimental data at

energies near and below the Coulomb barrier. The inclusion of breakup channel is found to be very essential and modifies the calculations of the total fusion cross section markedly and describes the experimental data very well below and above the Coulomb barrier[**35**].

- P. Eudes1, Z. Basrak2, et al in (2013) studied of nearly 300 fusion-evaporation cross section data reveals that, when properly scaled, fusion excitation function complies with a universal homographic law which is, within experimental errors, reaction system independent. From a such complete and summed complete and incomplete fusion excitation functions extracted are the limiting energy for the complete fusion and the main characteristics (onset, maximum and vanishing) of the incomplete fusion. The DYWAN microscopic transport model correctly predicts the incomplete fusion cross section for incident energies $\geq 15A$ MeV and suggests that the nuclear transparency is at the origin of fusion disappearance[**36**].

- V. Yu. Denisov in (2014) suggested that the full nucleus-nucleus potential consists of the macroscopic and shell correction parts. The deep sub-barrier fusion hindrance takes place in a nucleus-nucleus system with a strong negative shell-correction contribution to the full heavy-ion potential, while a strong positive shell-correction contribution to the full potential leads to weak enhancement of the deep sub-barrier fusion cross section[**37**].

1.3 Back ground of theory

Deuterium it is called heavy hydrogen, it is a stable isotope of hydrogen it is found in natural abundance in the oceans. Deuterium accounts for approximately 0.0156% of all naturally occurring hydrogen in the oceans on earth.

Tritium it is a radioactive isotope of hydrogen .The nucleus of tritium contains one proton and two neutrons. The most abundant hydrogen isotope of tritium is protium contains one proton and no neutrons. Naturally occurring tritium is rare on earth, where trace amounts are formed by the interaction of the atmosphere[15 liter][4]

In most fusion reactions two nuclei ($X1$ and $X2$) merge to form a heavier nucleus ($X3$) and a lighter particle ($X4$). To express this, we shall use either of the equivalent standard notations:

$X1 + X2 \rightarrow X^* \rightarrow X3 + X4$ ……. (1-1)

or

$X1(X2, X4)X3$. ……(1-2).

Due to conservation of energy and momentum, the energy released by the reaction is distributed among the two fusion products in quantity inversely proportional to their masses.

This indicate the velocities of the reacting nuclei in the laboratory system with $\mathbf{v}1$ and $\mathbf{v}2$, respectively, and their relative velocity with $\mathbf{v} = \mathbf{v}1 - \mathbf{v}2$. The center-of-mass energy of the system of the reacting nuclei is then:

$$\epsilon = \frac{1}{2} m_r v^2 \quad \text{……(1-3)}$$

where $v = |\mathbf{v}|$, and:

$$m_r = \frac{m_1 m_2}{m_1 + m_2} \quad \text{…….(1- 4)}$$

is the reduced mass of the system**[4]**.

Deuterium, tritium, neutron, and helium are the main players in the reaction (D + T = He + n + 17.6 MeV; see Figure (1.1) to realize the sun on

Earth. In the nanoworld of atoms and nuclei, particles exhibit wave characteristics, and nuclear properties and reaction mechanism are governed by the quantum mechanics theories.

These players have interesting properties. An encounter between deuterium and tritium results in the formation of a compound nucleus through the tunnel effect at a fractional energy of 500 keV Coulomb barrier potential. The compound nucleus has a high reaction probability near 80 keV due to the resonance phenomenon. In this way, nature gives humans a chance to use this reaction.[**5**]

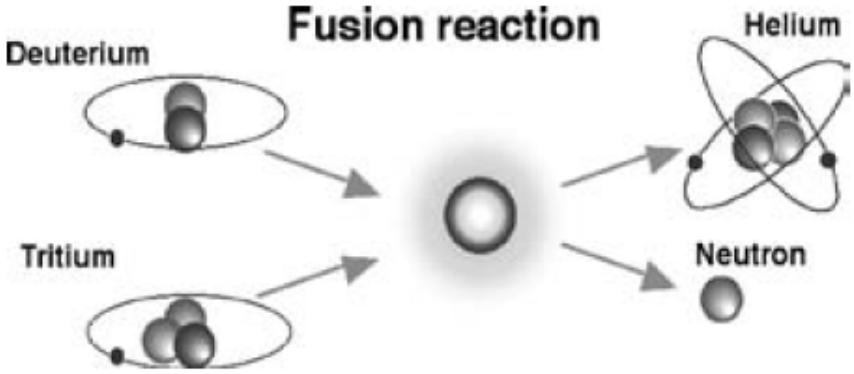

Figure (1.1) The fusion reaction.[5]

1.3.1 Fusion: Fusion of Little Nuts

The fusion that we are currently trying to achieve in ITER is the reaction of deuterium and tritium. This is different from the hydrogen fusion that takes place slowly in the sun. “Nucleus” is a Latin word meaning “little nuts”[**6**] . Deuterium and tritium form a “compound nucleus” (a concept originating from N. Bohr), ^{5}He (helium), when they get close enough to each other for the nuclear force to operate beyond the Coulomb barrier when

the distance r is less than 3 fermi if we use nuclear radius formula

r_n=1.25 $A^{1/3}$ fm (1 fermi =10^{-15} m; A is mass number)

as seen in Figure 1.2.

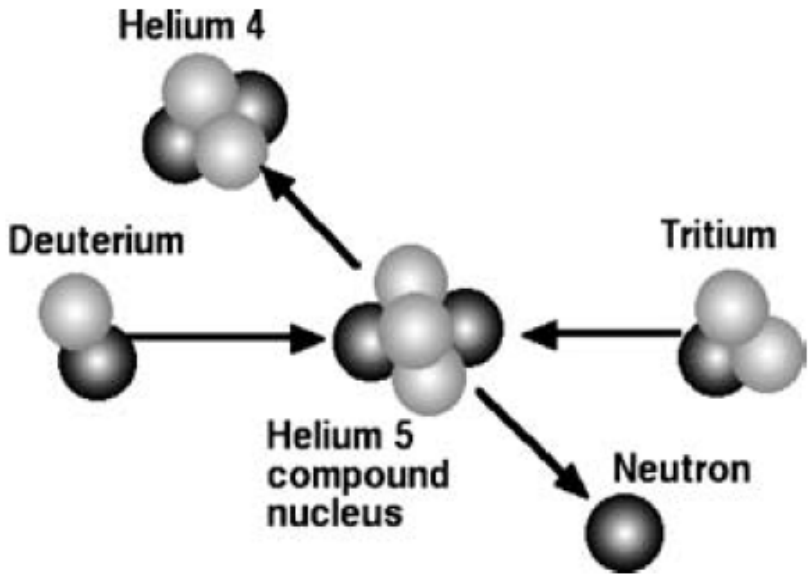

Figure (1.2) Schematic diagram of the DT fusion reaction via a compound nucleus .[5]

The kinetic energy of the incident nuclei is distributed to nuclei in the compound nucleus of deuterium and tritium. The neutron and helium, which have large energies, will, by chance, escape from compound nucleus.

D + T $\rightarrow {}^{5}_{2}He^{*} \rightarrow {}^{4}_{2}He$ + n +17.59 MeV …….(1- 5)

Let Umax be the barrier height for charged particles,

$U_{max} = e^2/(4\pi\epsilon_{\circ}r) = 0.48$ MeV **[5]**

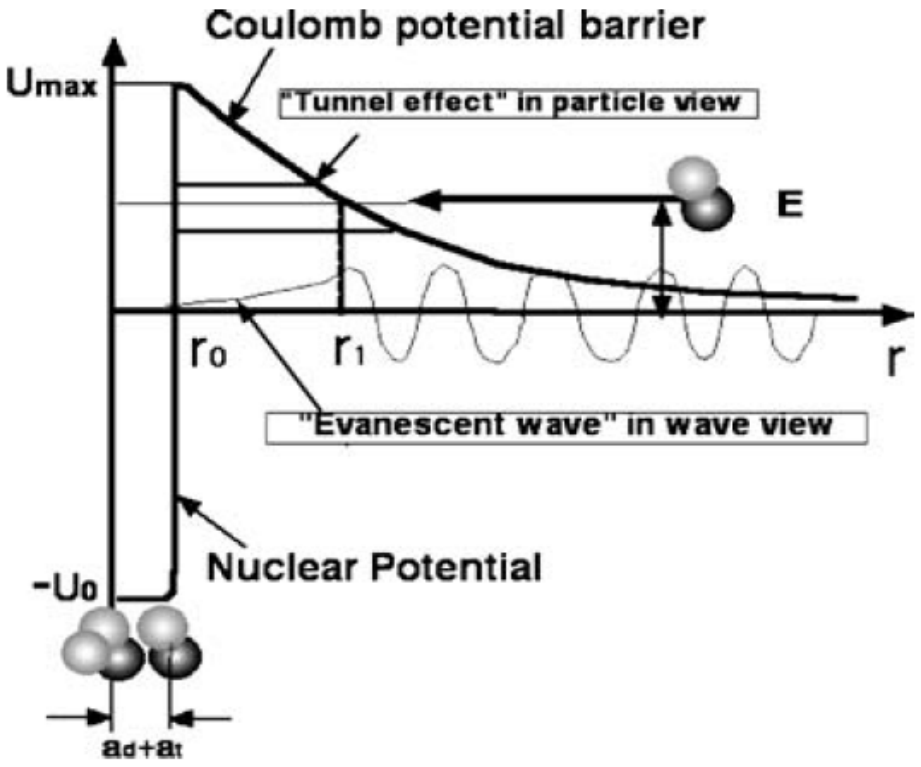

Figure (1.3) potential and wave function structure in the fusion reaction of deuterium and tritium.[5]

for r = 3 fermi as seen in Figure 1.3. Fusion will occur if the relative energy of deuterium and tritium is larger than 0.48 MeV, but it is difficult to raise the temperature to this level (3.7 billion degrees).

However, thanks to the wave nature of particles, fusion can occur at low energy (several 10 keV) by penetrating the Coulomb barrier. This is called the tunnel effect.

Scattering and penetration of the particle beam can be investigated by solving the Schrödinger equation under the Coulomb field (the potential

V = $e^2/(4\pi\epsilon_\circ r)$) . This Schrödinger equation was first derived by Austrian physicist Erwin Schrödinger (1887–1961) who was awarded the 1933 Nobel Prize in physics.[**5**]

1.4 Cross section, reactivity, and reaction rate

A most important quantity for the analysis of nuclear reactions is the *cross section*, which measures the probability per pair of particles for the occurrence of the reaction[**7**]. To be more specific, let us consider a uniform beam of particles of type '1', with velocity $v1$, interacting with a target containing particles of type '2' at rest. The cross section $\sigma_{12}(v_1)$ is defined as the number of reactions per target nucleus per unit time when the target is hit by a unit flux of projectile particles, that is, by one particle per unit target area per unit time. Actually, the above definition applies in general to particles with relative velocity v, and is therefore symmetric in the two particles, since we have $\sigma_{12}(v) = \sigma_{21}(v)$ **[4]**

Cross sections can also be expressed in terms of the centre-of-mass energy Eq (1.3), and we have $\sigma_{12}(\epsilon) = \sigma_{21}(\epsilon)$. In most cases, however, the cross sections are measured in experiments in which a beam of particles with energy ϵ_1, measured in the laboratory frame, hits a target at rest.

The corresponding beam-target cross-section $\sigma_{12}^{bt}(\epsilon_1)$ is releated to the centre of mass cross-section $\sigma_{12}(\epsilon)$ by **[4]**:

$$\sigma_{12}(\epsilon) = \sigma_{12}^{bt}(\epsilon_1) \qquad \ldots\ldots\ldots\ldots(1\text{-}6)$$

with $\epsilon_1 = \epsilon \cdot (m_1 + m_2)/m_2$ **[4]**

From now on, we shall refer to centre-of mass cross-sections and omit the indices 1 and 2.

If the target nuclei have density n_2 and are at rest or all move with the same velocity, and the relative velocity is the same for all pairs of projectile target nuclei, then the probability of reaction of nucleus '1' per unit path is given by the product $n_2\sigma(v)$. The probability of reaction per unit time is obtained by multiplying the probability per unit path times the distance v travelled in the unit time, which gives $n_2\ \sigma(v)v$.

Another important quantity is the *reactivity*, defined as the probability of reaction per unit time per unit density of target nuclei. In the present simple case, it is just given by the product σv. In general, target nuclei move, so that the relative velocity v is different for each pair of interacting nuclei. In this case, we compute an expected value **[4]:**

$$<\sigma v> = \int_0^\infty \sigma(v) v f(v) dv \qquad \text{.....(1- 7)}$$

where $f(v)$ is the distribution function of the relative velocities, normalized in such a way that $\int_0^\infty f(v)dv = 1$. It is to be observed that when projectile and target particles are of the same species, each reaction is counted twice.

Both controlled fusion fuels and stellar media are usually mixtures of elements where species '1' and '2', have number densities n_1 and n_2, respectively. The volumetric *reaction rate*, that is, the number of reactions per unit time and per unit volume is then given by:

$$R_{12} = \frac{n_1 n_2}{1+\delta_{12}} <\sigma v> = \frac{f_1 f_2}{1+\delta_{12}} n^2 <\sigma v> \qquad \text{.....(1- 8)}$$

Here *n* is the total nuclei number density and *f*1 and *f*2 are the atomic fractions of species '1' and '2', respectively. The Kronecker symbol δij (with $\delta ij = 1$, if $i = j$ and $\delta ij = 0$ elsewhere) is introduced to properly take into account the case of reactions between like particles. Equation 1.8 shows a very important feature for fusion energy research: the volumetric reaction rate is proportional to the square of the density of the mixture. For future reference, it is also useful to recast it in terms of the mass density ρ of the reacting fuel:

$$R_{12} = \frac{f_1 f_2}{1+\delta_{12}} \frac{\rho^2}{\bar{m}^2} <\sigma v> \qquad \text{.....(1- 9)}$$

where $\bar{m}^2$ is the average nuclear mass. Here, the mass density is computed as $\rho = \sum j\ njmj = n\ \bar{m}^2$, where the sum is over all species, and the very small contribution due to the electrons is neglected.We also immediately see that the specific reaction rate, that is, the reaction rate per unit mass, is proportional to the mass density, again indicating the role of the density of the fuel in achieving efficient release of fusion energy[**4**].

1.5 Nuclear Potential

In general, nuclear reaction is usually theorized and analyzed in three steps; initial state interaction, intermediate compound state and final state interaction. Transition from intermediate state to final state has various, sometimes complex, channels such as the electro-magnetic transition to ground state emitting gamma rays, the particle (neutron, proton, alpha-particle etc.) emission and residual nucleus, which sometimes decay to ground state emitting gamma-rays, and the direct break-up to two or more

nuclei like fission. Potential for nuclear strong force and Coulomb force in these cases can be categorized into three cases[**8**]) as in fig.(1-4).

The potential state (I) shows the case that nucleons (neutrons and protons) are trapped in a very deep well of strong force. Stable isotopes of masses less than 60 have this type potential well. Fusion reactions by two light nuclei produce stable isotopes of this type.

The potential state (II) appears for intermediate compound state in general. Radioactive isotope has this kind of potential. Stable isotopes having masses greater than 60 are trapped in these type potentials which are drawn according to the fission channels breaking-up to lighter nuclei. In this case, the depth of trapping potential is deep enough to have very long life time, but positive Q-value for fission channels makes height of potential tail in outer-skirt lower than the depth of trapping well. At ground state, the thickness of potential well is large enough to make the quantum-mechanical tunneling probability of fission to be "inverse-astronomically" very close to zero.Therefore, nucleus is regarded as stable isotope. Here, Q-value is obtained by calculating mass defect between before and after reaction, using Einstein's formula $E = mc^2$[**9**]. However, when the intermediate compound nucleus has high inner excited energy Ex, the thickness of outer wall of trapping potential becomes relatively thin and quantum mechanical tunneling probability for particle emission or fission can dramatically increase. Fission process for uranium and trans-uranium nuclei is induced in this way. Moreover, we may have possibility of fission for lighter nuclei with mass $A < 200$. In some of proposed theories[**10-12**]) in the Condensed Matter Nuclear Science (CMNS), deterministic models of fission for $60 < A < 200$ nuclei have been developed**[9]**.

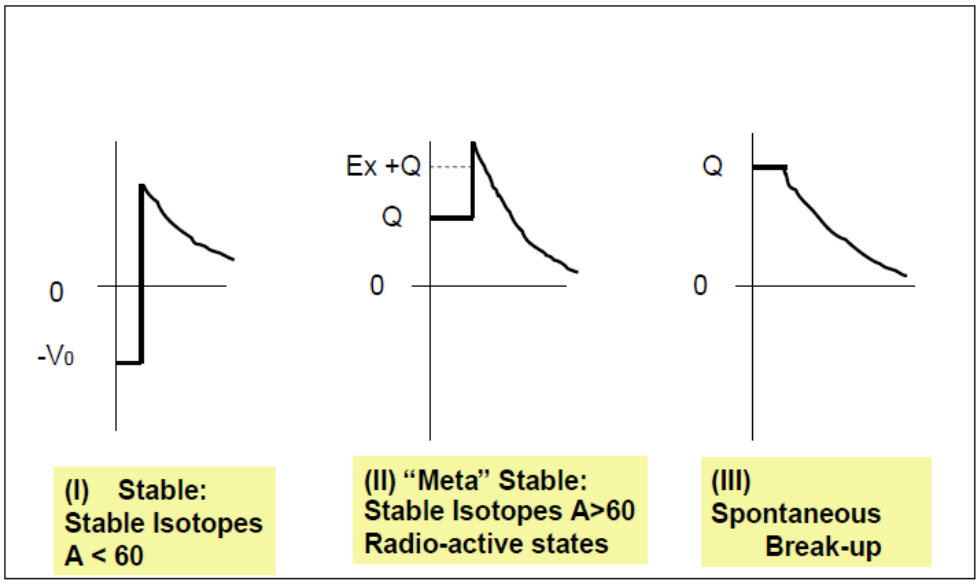

Figure (1-4): Three potential types for nuclear interaction[9].

The potential type (III) is the case for intermediate compound nucleus having very high inner excited energy Ex, such as cases of fusion reactions of hydrogen isotopes. Compound nucleus in this case promptly breaks up to fragment-particles.[**9**]

1.5.1 Strong Interaction

Now we explain very briefly the feature of potential by nuclear strong interaction. The reason why nucleons are trapped within very small spherical space with radius about 5 fm (1 fm = 110^{-15} m) was first solved by the famous Yukawa model of pion exchange. Hideki Yukawa won Nobel Prize by this theory. Later, the theory of strong force has been deepened by the development of QCD[**13**]) based on concept of quark and gluon. However, as the conclusion in recent views of nuclear physics, the strong interaction can be drawn accurately enough by the Yukawa model with charged pions ($\pi +,\pi—$) and neutral pion, for relative reaction energy less than about 200

MeV (less than the threshold energy of pion-generation). Especially, for fusion reaction process, charged pions play role of sticking two (or more) nuclei. Nuclear fusion by strong interaction can be simulated by the catch-ball model of charged pions between nuclei for fusing. Due to the very short range of de Broglie wave length (about 2 fm) of pion, the strong interaction for fusion becomes very short range force, namely "almost on surface" sticking force. For example, when relatively large (A>6) two nuclei approach closely, fusion force by exchanging charged pions (between neutron and proton for counter-part nuclei) becomes the sticking force near at surface (R= $r_\circ$). Exchange of neutral pion for scattering (repulsive) force between nucleons of counter-part nuclei also happens in the region relatively near at surface. Especially, nuclear fusion reactions at very low energy as cold cluster fusion and transmutation as modeled by EQPET/TSC theory , largeness of surface area for exchanging charged pions governs the largeness of reaction cross section. This is specific character of "nuclear reactions in condensed matter"[**9**].

1.5.2 Optical Potential

Global optical potential [**14**]), written by complex number, is used for nuclear potential of strong interaction for scattering and sticking forces. Image of global optical potential is drawn in Fig.1-5. The real part, namely deep trapping potential V(r) is a well with rather round shape near at surface of nucleus (Woods-Saxon type) , but is approximated to be constant value $V_\circ$ within in nucleus.

$$U(r) = V(r) + i\, W(r) \qquad \text{……(1- 10)}$$

$V_\circ$ is about -25MeV for deuteron. $V_\circ$ value saturates to about -50MeV for nuclei of A>24. Imaginary part W(r) corresponds to the interaction of charged-pion exchange, and locates near at surface (r = $r_\circ$) to be approximated by delta-function $W_\circ\delta$(r- $r_\circ$). When we use this delta-function approximation, fusion rate formula becomes simple[**9**].

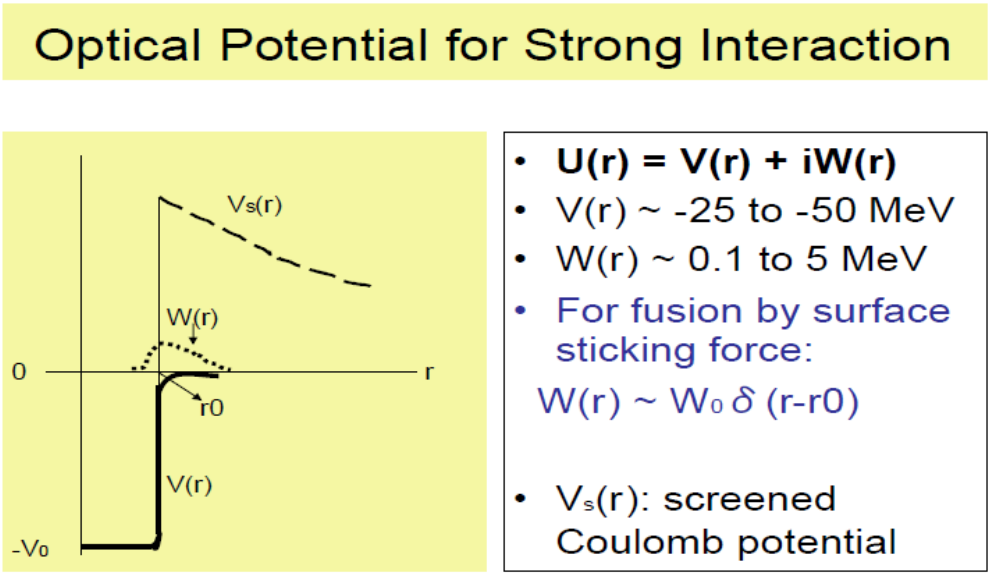

Figure(1-5): Optical potential for strong interaction[9]

T Matrix and Reaction Cross Section

Now we briefly summarize quantum mechanical basis of scattering and reaction process.

Asymptotic wave function [**14,15**]) after scattering (interaction) is written by Eq.(1-11).

$$\Psi(r) \approx e^{ikz} + f(\theta)(e^{ikr} / r) \qquad \text{.....(1-11)}$$

Differential cross section of process is defined by**:**

$\frac{d\sigma}{d\Omega} = |f(\theta)|^2$ ……..(1-12)

S-matrix is defined by the phase-shift analysis [**14,15**]) as using Legendre polynomial expansion for scattering amplitude $f(\theta)$

$f(\theta) = (1/2ik) \sum_{l=0}^{\infty}(2l+1)(S_l - 1)P_l(\cos\theta)$ ……..(1-13)

$S_l = e^{2i\delta_l}$ ……...(1-14)

In general reaction process, not only elastic scattering but also absorption, fusion, particle emission processes are taking place as transition. To treat the transition from (α, β) to (α', β') channel, evaluation of T-matrix elements are usually done. T-matrix is defined by the following Lippmann-Schwinger equation[**15**]:

$T = U + UG_\circ T$ ……..(1-15)

$G_\circ = (E - H_\circ + I\delta)^{-1}$ ……..(1-16)

$H = U + H_\circ$ ……...(1-17)

Here, $G_\circ$ is the Green operator for H0 Hamiltonian with kinetic energy and spin Hamiltonian only. Scattering amplitude is defined by:

$f(\theta; \alpha\beta \rightarrow \alpha'\beta') = -(2\pi/h^2) < \Psi_{\alpha'\beta'} |T| \Psi_{\alpha\beta} >$ ……(1-18)

If we approximate T=T(0) = U, formula (1-18) becomes the Born approximation. Lippmann-Schwinger equation can be regarded as an integral type equation of Schroedinger differential equation. The first order approximation of T is given by inserting T=U in Eq (1-15), and we obtain $T(1) = U + UG_\circ U$. The second order approximation is then given as T(2) =

U + U$G_{\circ}$T(1) , and the n-th order approximation gives T(n) = U +U$G_{\circ}$T(n-1) . This successive treatment is known as Neumann series solution of integral equation[**16**].

We can treat reaction cross section including transition by evaluating T matrix elements.

For the optical potential of V + iW type with constant V and W values, formulas of reaction cross section are given in standard text book of nuclear physics(Chapter 9 of Reference 6) for S-wave (l =0).

$$\sigma_{r.0} = \pi\lambda^2 \frac{-4KRIm\ f_{\circ}}{(Ref_{\circ})^2+(Imf_{\circ}-KR)^2} \quad \text{.....(1-19)}$$

$$K = \frac{1}{\hbar}\sqrt{2M(|E+V+iW|)} \quad \text{.....(1-20)}$$

$$f_{\circ} = KR\ cotKR \quad \text{.....(1-21)}$$

And relations between S-matrix and T-matrix for Legendre coefficients are[3]:

$$T_l = e^{i\delta_l} \sin\delta_l \quad \text{.....(1-21)}$$

$$S_l = 1+2iT_l \quad \text{.....(1-22)}$$

By evaluating T-matrix elements, we can treat reaction with channel transition.

As shown in Fig.1-6 , X. Z. Li evaluated fusion cross section for dd, dt and d ^3He reactions using S-matrix formulas. Fusion cross sections are shown in Fig.1-6. S-matrix formula and evaluated values of V and W (written as U_{1r} and U_{1i} in Fig.1-4) for dt reaction are shown in Fig.1-6.[3]

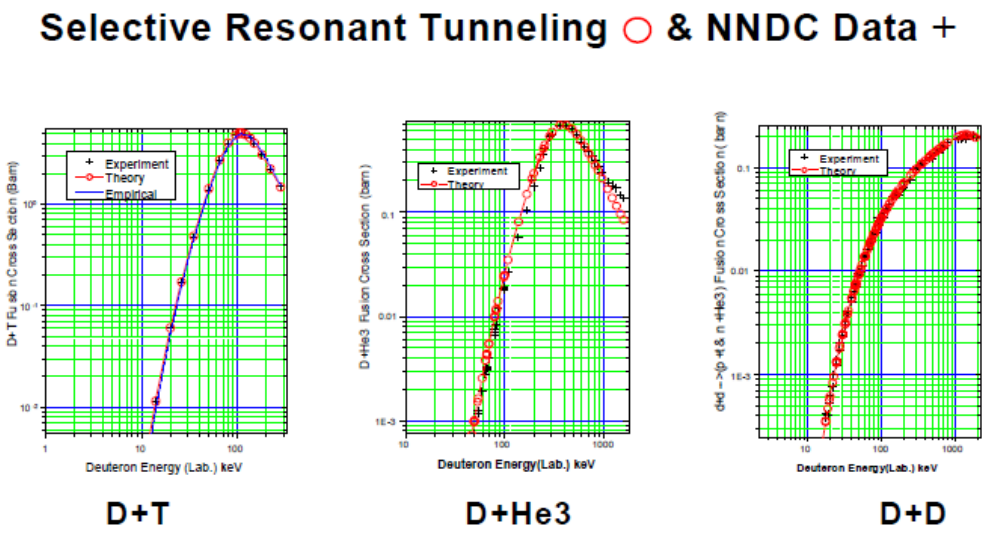

Figure (1-6): Fusion cross sections for dt, d3He and dd processes.[3]

Li used the reaction cross section formula with S-matrix [**17**]. Li obtained averaged values of V and W of optical potential by fitting calculated curves to experimental cross sections.[3]

Finally We know that Fusion, a source of the sun's energy offer a clean, potentially limitless source of electricity and power. Hence a magnetic fusion reactor by using plasma would manage to bring about the nuclear fusion reation in a controlled way. Plasma is a new state of matter in which most of the atoms are ionized due to some sort of `violence' and breaking away of the originally bound electrons.Within the plasma, colliding deuterium and tritium nuclei would fuse into helium nuclei and release energy to be converted into electricity.

1.6 Aim of present work:

Calculation the cross section for controlled fusion reactions play important rule in the design of any nuclear fusion systems requires prior theoretical calculations to identify all the relevant physical factors such as

the neutron and proton and x-ray yields in addition to the reaction rate where from these factors one can bring to the find requirement calculation for calculation the electric power generation.

Chapter 2

Theory

2.1 Fusion cross section parametrization

In order to fuse, two positively charged nuclei must come into contact, winning the repulsive Coulomb force. Such a situation is made evident by the graph of the radial behaviour of the potential energy of a two nucleon system, shown in Fig. 2.1. The potential is essentially Coulombian and repulsive

$$V_{c(r)} = \frac{Z_1 Z_2 e^2}{r} \qquad \text{.....(2-1)}$$

at distances greater than

$r_n \cong 1.44\ (A_1{}^{1/3} + A_2{}^{1/3})$ fermi ……..(2-2)

which is about the sum of the radii of the two nuclei. In the above equations z_1 and z_2 are the atomic numbers, A_2 and A_2 the mass numbers of the interacting nuclei, and *e* is the electron charge. At distances $r < r_n$ the two nuclei feel the attractive nuclear force, characterized by a potential well of depth $U_\circ$ = 30– 40 MeV.

Using eqns 2.1 and 2.2 we find that the height of the Coulomb barrier

$$V_b \approx V_c(r_n) = \frac{Z_1 Z_2}{A_1{}^{1/3} + A_2{}^{1/3}}\ \text{MeV} \qquad \text{…….(2-3)}$$

is of the order of one million electron-Volts (1 MeV). According to classical mechanics, only nuclei with energy exceeding such a value can overcome

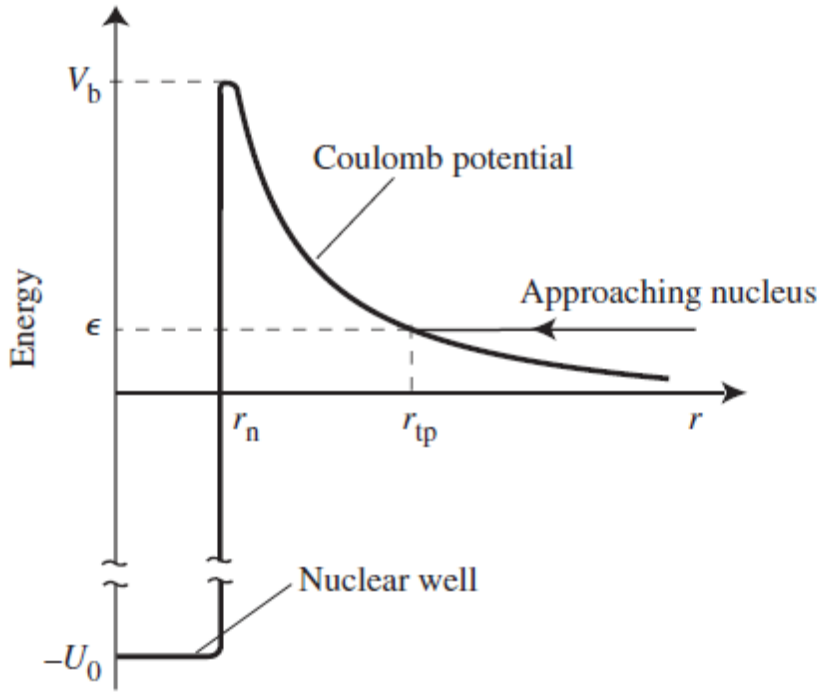

Figure (2.1) Potential energy versus distance between two charged nuclei approaching each other with center-of-mass energy _. The figure shows the nuclear well, the Coulomb barrier, and the classical turning point[4].

the barrier and come into contact. Instead, two nuclei with relative energy ϵ $<V_b$ can only approach each other up to the classical turning point

$$r_{tp} = \frac{Z_1 Z_2 e^2}{\epsilon} \qquad \text{.....(2-4)}$$

Quantum mechanics, however, allows for *tunnelling* a potential barrier of finite extension, thus making fusion reactions between nuclei with energy smaller than the height of the barrier possible.

A widely used parametrization of fusion reaction cross-sections is[4]

$$\sigma \approx \sigma_{geom} \times T_l \times R, \qquad \text{……(2-5)}$$

where σ_{geom} is a geometrical cross-section, *T* is the barrier transparency, and *R* is the probability that nuclei come into contact fuse. The first quantity is of the order of the square of the de-Broglie wavelength of the system[4]:

$$\sigma_{geom} \approx \lambda\!\!\!^{-2} = \left(\frac{\hbar}{m_r v}\right)^2 \propto \frac{1}{\epsilon} \qquad \ldots\ldots\ldots(2\text{-}6)$$

where ħ is the reduced Planck constant and m_r is the reduced mass . Concerning the barrier transparency, we shall see that it is often well approximated by[4]:

$$T_l \approx T_G = \exp\left(-\sqrt{\epsilon_G/\epsilon}\right) \qquad \ldots\ldots\ldots(2\text{-}7)$$

which is known as the Gamow factor (after the scientist who first computed it), where:

$$\epsilon_G = (\pi\, \alpha_f Z_1 Z_2\,)^2\, 2m_r c^2 = 986.1\, Z_1^{\,2} Z_2^{\,2}\, A_r \text{ (keV)} \ldots.(2\text{-}8)$$

is the Gamow energy, $\alpha_f = e^2/\hbar c = 1/137.04$ is the fine-structure constant commonly used in quantum mechanics, and $A_r = m_r/m_p$. Equation 2.7 holds as far as $\epsilon \ll \epsilon_G$, which sets no limitations to the problems we are interested in Eq(2.7) and 2.8 show that the chance of tunnelling decreases rapidly with the atomic number and mass, thus providing a first simple explanation for the fact that fusion reactions of interest for energy production on earth only involve the lightest nuclei the reaction characteristics contains essentially all the nuclear physics of the specific reaction. It takes substantially different values depending on the nature of the interaction characterizing the reaction. It is largest for reactions due to

strong nuclear interactions; it is smaller by several orders of magnitude for electromagnetic nuclear interactions; it is still smaller by as many as 20 orders of magnitude for weak interactions. For most reactions, the variation of $R(\epsilon)$ is small compared to the strong variation due to the Gamow factor. Astrophysical *S* factor in conclusion, the cross section is often written as[4]:

$$\sigma(\epsilon) = \frac{S(\epsilon)}{\epsilon} \exp\left(-\sqrt{\epsilon_G/\epsilon}\right) \qquad \ldots\ldots(2\text{-}9)$$

where the function $S(\epsilon)$ is called the *astrophysical S factor*, which for many important reactions is a weakly varying function of the energy. An excellent introduction to the computation of fusion cross-sections and thermonuclear reaction rates can be found in the classical textbook on stellar nucleosynthesis by Clayton (1983). Classic references on nuclear physics are Blatt and Weisskopf (1953), Segrè (1964), and Burcham (1973). In the following portion of this section, we outline the evaluation of the fusion cross-section for non-resonant reactions, which justifies the parametrization 2.9. The treatment is simplified and qualitative, but still rather technical[**4**]

2.1.1 Penetration factors for non-resonant reactions

The total cross-section can be obtained as a sum over partial waves, that is over the contributions of the different terms of an expansion of the particle wave-function in the components of the angular momentum *l*. We then write**[7]**:

$$\rho(v) = \sum_l \sigma_l(v) \qquad \ldots\ldots(2\text{-}10)$$

Far from resonances the partial cross-section can be put in the form[7]:

$$\sigma_l(v) \approx 2\pi\lambda\!\!\!^{-2}\,(2l+1)\beta_l \mathrm{T}_l \qquad \ldots\ldots(2\text{-}11)$$

where β_l is a function taking into account nuclear interactions and T_l is the barrier transmission coefficient. This last factor, defined as the ratio of particles entering the nucleus per unit time to the number of particles incident on the barrier per unit time, can be written as[7]:

$$\mathrm{T}_l \approx P_l\left(1+\frac{\lambda\!\!\!^{-2}}{\lambda\!\!\!^{-2}_{\circ}}\right)^{-1/2} = P_l\left(1+\frac{U_\circ}{\epsilon}\right)^{-1/2} \approx \left(\frac{\epsilon}{U_\circ}\right)^{1/2} P_l \quad \ldots..(2\text{-}12)$$

that is, the product of the barrier penetration factor P_l , measuring the probability that nucleus '2' reaches the surface of nucleus '1', and of a potential discontinuity factor, due to the difference between the wavelength of the free nucleus and that of the compound nucleus in the nuclear well $\lambda\!\!\!^{-}_{\circ} = \hbar/(2m_r U_\circ)^{1/2}$. According to quantum mechanics, the barrier penetration factors P_l are computed by solving the time-independent Schroedinger equation[7]:

$$\frac{\hbar^2}{2m_r}\nabla^2\Psi + (\epsilon - V_c)\,\Psi = 0 \qquad \ldots\ldots.(2\text{-}13)$$

for the wavefunction $\psi(\mathbf{r})$ describing the relative motion of the two interacting nucleons in a Coulomb potential extending from $r = 0$ to infinity.

As usual for problems characterized by a central potential, we separate radial and angular variables, that is, we write $\psi(r, \theta, \varphi) = Y(\theta, \varphi)\chi(r)/r$. We then expand the function $\chi(r)$ into angular momentum components, $x_l(r)$, each satisfying the equation[7]:

$$\frac{1}{r^2}\frac{d}{dr}\frac{d^2}{dr^2}x_l(\mathrm{r}) + \frac{2m_r}{\hbar^2}[\epsilon - W_l(\mathrm{r})]x_l(\mathrm{r}) = 0 \qquad \text{……..(2-14)}$$

Where

$$W_l(\mathrm{r}) = V_{c(r)} + \frac{\hbar^2 l(l+1)}{2m_r r^2} \qquad \text{…….(2-15)}$$

takes the role of an effective potential for the *l*th component. This last equation shows that each angular momentum component sees an effective potential barrier of height increasing with *l*.We therefore expect the $l = 0$ component (*S*-wave) to dominate the cross section, in particular for light elements. An exception will occur for reactions in which the compound nucleus, formed when the two nuclei come into contact, has forbidden $l = 0$ levels. This latter case, however, does not occur for any reaction of relevance to controlled fusion.

Once the solution $x_l(r)$ of Eq(2.14) is known, the penetration factor for particles with angular momentum *l* is given by[7]:

$$P_l = \frac{x_l{}^*(r_n)x_l r_n}{x_l{}^*(\infty)x_l(\infty)} \qquad \text{…….(2-16)}$$

Exact computations of the wavefunctions $x_l(r)$ are feasible, but involved (Bloch *et al.* 1951). However, much simpler and yet accurate evaluations of

the penetration factors can be performed by means of WKB method (after the initials of Wentzel, Kramers, and Brillouin), discussed in detail in standard books on quantum mechanics (Landau and Lifshitz 1965; Messiah 1999) or mathematical physics (Matthews and Walker 1970). A pedagogical application to the computation of penetration factors is presented by Clayton (1983). Here it suffices to say that application of the method leads to[7]

$$P_l = \left[\frac{W_l(r_n) - \epsilon}{\epsilon}\right]^{1/2} \exp(-G_l) \qquad \text{.....(2-17)}$$

with the dominant exponential factor given by[7]:

$$G_l = 2\frac{(2m_r)^{1/2}}{\hbar} \int_{r_n}^{r_{tp}(\epsilon)} [W_l(r) - \epsilon]^{1/2}\, dr \qquad \text{.....(2-18)}$$

where r_{tp} is the turning point distance (2.4). For $l = 0$, using Eq(2.15) for $W_l(r)$, we obtained [7]:

$$G_\circ = \frac{2}{\pi}\sqrt{\frac{\epsilon_G}{\epsilon}}\left[arccos\sqrt{\frac{r_n}{r_{tp}}} - \sqrt{\frac{r_n}{r_{tp}}}\sqrt{1 - \frac{r_n}{r_{tp}}}\right] \qquad \text{.....(2-19)}$$

Since for Eq(2.3) (2.4), $r_n/r_{tp}\ (\epsilon) = \epsilon/V_b$, and in the cases of interest $\epsilon << V_b$, we can expand the right-hand side of Eq (2.19) in powers of (ϵ/V_b), thus obtaining[7]:

$$G_\circ = \sqrt{\frac{\epsilon_G}{\epsilon}}\left[1 - \frac{4}{\pi}\left(\frac{\epsilon}{V_b}\right)^{1/2} + \frac{2}{3\pi}\left(\frac{\epsilon}{V_b}\right)^{3/2} + \cdots\right] \qquad \text{.....(2-20)}$$

In the low energy limit, we have $G_\circ \approx (\epsilon_G/\epsilon)^{1/2}$, and the *S*-wave penetration factor becomes[7]:

$$P_\circ \cong \left(\frac{V_b}{\epsilon}\right)^{1/2} \exp\left(-\sqrt{\frac{\epsilon_G}{\epsilon}}\right) \qquad \text{.....(2-21)}$$

Penetration factors for $l > 0$ are approximately given by[7]:

$$P_l = P_\circ \exp\left[-2l(l+1)\left(\frac{V_l}{V_b}\right)^{1/2}\right]$$

$$= P_\circ \exp\left[-7.62l(l+1)/(A_r r_{nf} Z_1 Z_2)^{1/2}\right] \qquad \text{.....(2-22)}$$

where r_{nf} is the nuclear radius in units of 1 fermi = 10^{-15}cm. Equation 2.22 confirms that angular momentum components with $l > 0$ have penetration factors much smaller than the $l = 0$ component. This allows us to keep the *S*-wave term only in the cross-section expansion in Eq(2.10), which leads us to evaluate the barrier transparency and the cross section as[7]:

$$T_l \approx \mathrm{T}_\circ = \left(\frac{V_b}{U_\circ}\right)^{1/2} \exp\left(-\sqrt{\frac{\epsilon_G}{\epsilon}}\right) \qquad \text{.....(2-23)}$$

And

$$\sigma(\epsilon) \approx \sigma_l = 0(\epsilon) \approx \left[\pi \frac{\hbar^2}{m_r} \beta_l = 0 \left(\frac{V_b}{U_\circ}\right)^{1/2}\right] \frac{\exp(-\epsilon_G/\epsilon)}{\epsilon} \quad \text{.....(2-24)}$$

respectively. Equation 2.24 for the cross section has the same form as the parametrization Eq(2.9), with the term in square brackets corresponding to the astrophysical *S*-factor. *S*-wave cross section.

Another form of Eq (2.23), which will turn useful later, is[7]:

$$T_l = \left(\frac{V_b}{U_\circ}\right)^{1/2} exp\left[-\pi\left(\frac{r_{tp}}{a_B{}^*}\right)^{1/2}\right] \quad \text{.....(2-25)}$$

Where

$$a_B{}^* = \hbar^2/(2m_r Z_1 Z_2 e^2) \quad \text{.....(2-26)}$$

may be looked at as a nuclear Bohr radius[**7**].

2.2 Some important fusion reactions

In Table 2.1 we list some fusion reactions of interest to controlled fusion research and to astrophysics. For each reaction the table gives the*Q*-value, the zero-energy astrophysical factor *S(*0*)* and the square root of the Gamow energy ϵ_G. For the cases in which *S(*ϵ*)* is weakly varying these data allow for relatively accurate evaluation of the cross section, using eqn 2.9, with *S* = *S(*0*)*.

For some of the main reactions, Table 2.2 gives the measured cross sections at ϵ = 10 keV and ϵ = 100 keV, as well as the maximum value of

the cross-section σ_{max} , and the energy ϵ_{max} , at which the maximum occurs. Also shown, in parentheses, are theoretical data for the pp and CC reactions. In the tables and in the following discussion, the reactions are grouped according to the field of interest.

A large and continuously updated database on fusion reactions, quoting original references for all included data, has been produced and is updated by the NACRE (Nuclear Astrophysics Compilation of Reaction rates) group (Angulo *et al*. 1999) and can also be accessed through the internet . Standard references for fusion reaction rates are a compilation of data by Fowler *et al*. (1967) and its subsequent updates (Fowler *et al*. 1975; Harris *et al*. 1983). Data on many fusion reactions of astrophysical relevance have been recently reviewed by Adelberger *et al*. (1998). Data on the DD, DT, and D 3He reactions have been critically reviewed by Bosch and Hale (1992); the most recent reference on p 11B is Nevins and Swain (2000). An interesting list of thermonuclear reactions has also been published by Cox *et al*. (1990). Graphs of the cross section of reactions of interest to fusion energy versus center-of-mass energy are shown in Fig. 2.2.[**7**]

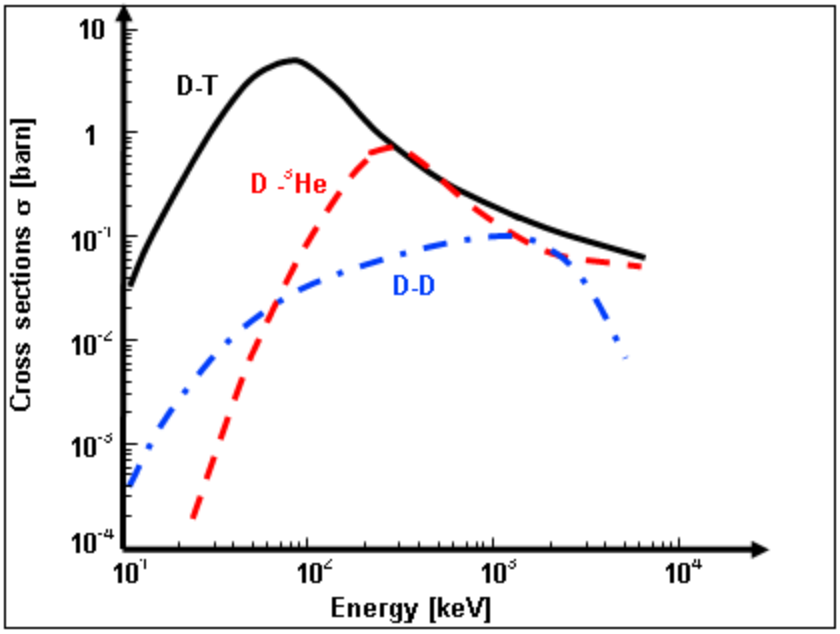

Figure(2.2)Fusion cross sections versus centre-of-mass energy for reactions of interest to controlled fusion energy [38].

2.2.1 Main controlled fusion fuels

First, we consider the reactions between the hydrogen isotopes deuterium and tritium, which are most important for controlled fusion research. Due to Z = 1, these hydrogen reactions have relatively small values of ϵ_G and hence relatively large tunnel penetrability. They also have a relatively large S.

The DT reaction:

$$D + T \rightarrow \alpha\ (3.5\ MeV) + n\ (14.1\ MeV) \qquad \text{.....(2-27)}$$

has the largest cross-section, which reaches its maximum (about 5 barn) at the relatively modest energy of 64 keV (see Fig. 2.2). Its Q_{DT} = 17.6 MeV is the largest of this family of reactions. It is to be observed that the cross

Table (2.1) Some important fusion reactions and parameters of the cross-section factorization [4]

	Q (MeV)	$\langle Q_v \rangle$ (MeV)	S(0) (keV barn)	$\epsilon_G^{1/2}$ ($keV^{1/2}$)
Main controlled fusion fuels				
$D+T \longrightarrow \alpha + n$	17.59		1.2×10^4	34.38
$D + D \longrightarrow$ T+P	4.04		56	31.40
$D + D \longrightarrow {}^3He + n$	3.27		54	31.40
$D + D \longrightarrow \alpha + \gamma$	23.85		4.2×10^{-3}	31.40
$T + T \longrightarrow \alpha + 2n$	11.33		138	38.45
Advanced fusion fuels				
$D + {}^3He \longrightarrow \alpha + p$	18.35		5.9×10^3	68.75
$p + {}^6Li \longrightarrow \alpha + {}^3He$	4.02		5.5×10^3	87.20
$p + {}^7Li \longrightarrow 2\alpha$	17.35		80	88.11
$p + {}^{11}B \longrightarrow 3\alpha$	8.68		2×10^5	150.3
the p-p cycle				
$p + p \longrightarrow D + e^+ + \upsilon$	1.44		4.0×10^{-22}	22.20
$D + p \longrightarrow {}^3He + \gamma$	5.49	0.27	2.5×10^{-4}	25.64
${}^3He + {}^3He \longrightarrow \alpha + 2p$	12.86		5.4×10^3	153.8
CNO cycle				
$p + {}^{12}C \longrightarrow {}^{13}N + \gamma$	1.94		1.34	181.0
$[{}^{13}N \longrightarrow {}^{13}C + e^+ + \upsilon + \gamma]$	2.22		–	–
$p + {}^{13}C \longrightarrow {}^{14}N + \gamma$	7.55	0.71	7.6	181.5
$p + {}^{14}N \longrightarrow {}^{15}O + \gamma$	7.29		3.5	212.3
$[{}^{15}O \longrightarrow {}^{15}N + e^+ + \upsilon + \gamma]$	2.76	1.00	—	–
$p + {}^{15}N \longrightarrow {}^{12}C + \alpha$	4.97		6.75×10^4	212.8
Carbon burn				
$^{12}C + C^{12} \longrightarrow {}^{23}Na + p$	2.24			
$^{12}C + C^{12} \longrightarrow {}^{20}Na + \alpha$	4.62		8.83×10^{19}	2769
$^{12}C + C^{12} \longrightarrow {}^{24}Mg + \gamma$	13.93			

The Q^*value includes both positron disintegration energy and neutrino energy, when relevant. The quantity $\langle Q_v{}^* \rangle$ is the average neutrino energy. As usual in nuclear physics, cross sections are expressed in barn; 1 barn = $10^{-24} cm^2$

Table (2.2): fusion reaction cross section at the centre of mass energy of 10keV and 100keV. Maximum cross –section σ_{max} and location of the maximum E_{max}. Values in parentheses are estimated theoretically; all others are measured data [4].

Reaction	σ(10keV) (barn)	σ(100keV) (barn)	σ_{max} (barn)	ϵ_{max} (keV)
$D + T \rightarrow {}^{5}_{2}C^{*} \rightarrow \alpha + n$	2.72×10^{-2}	3.43	5.0	64
$D + D \rightarrow {}^{4}_{2}C^{*} \rightarrow T + p$	2.81×10^{-4}	3.3×10^{-2}	0.096	1250
$D + D \rightarrow {}^{4}_{2}C^{*} {}^{3}He + n$	2.78×10^{-4}	3.7×10^{-2}	0.11	1750
$T + T \rightarrow {}^{6}_{2}C^{*} \rightarrow \alpha + 2n$	7.90×10^{-4}	3.4×10^{-2}	0.16	1000
$D + {}^{3}He \rightarrow {}^{5}_{3}C^{*} \rightarrow \alpha + p$	2.2×10^{-7}	0.1	0.9	250
	6×10^{-10}	7×10^{-3}	0.22	1500
$p + {}^{6}Li \rightarrow {}^{7}_{4}C^{*} \rightarrow \alpha + {}^{3}He$	(4.6×10^{-17})	3×10^{-4}	1.2	550
	(3.6×10^{-26})	(4.4×10^{-25})		
$p + {}^{11}B \rightarrow {}^{12}_{6}C^{*} \rightarrow 3\alpha$	(1.9×10^{-26})	2.0×10^{-10}	1.0×10^{-4}	400
$p + p \rightarrow {}^{2}_{2}C^{*} \rightarrow D + e+ + \nu$		(5.0×10^{-103})		
$p + {}^{12}C \rightarrow {}^{13}_{7}C^{*} \rightarrow {}^{13}N + \gamma$				

section of this reaction is characterized by a broad resonance for the formation of the compound ${}^{5}He$ nucleus at $\epsilon \approx$ 64 keV. Therefore, the astrophysical factor *S* exhibits a large variation in the energy interval of interest.

The DD reactions:

$$D + D \rightarrow T + P + 4.04\ MeV \qquad \text{.....(2-28)}$$

$$D + D \rightarrow {}^{3}_{2}He + n + 3.27\ MeV \qquad \text{.....(2-29)}$$

Are nearly equiprobable. In the 10–100 keV energy interval, the cross sections for each of them are about 100 times smaller than for DT. The reaction$D(d, \gamma)\,{}^{4}He$, instead has cross section about 10,000 times smaller than that of 2.28 and 2.29.

The TT reaction has cross section comparable to that of DD. Notice that since the reaction has three products, the energies associated to each of them are not uniquely determined by conservation laws.[**4**]

2.3 Maxwell-averaged fusion reactivities

As we have seen earlier, the effectiveness of a fusion fuel is characterized by its reactivity $<\sigma v>$. Both in controlled fusion and in astrophysics we usually deal with mixtures of nuclei of different species, in thermal equilibrium, characterized by Maxwellian velocity distributions[4]:

$$f_j(v_j) = \left(\frac{m_j}{2\pi k_B T}\right)^{3/2} \exp\left(-\frac{m_j {v_j}^2}{2k_B T}\right) \qquad \text{.....(2-30)}$$

Where the subscript j labels the species, T is the temperature and k_B is Boltzmann constant. The expression for the Eq (1.7) can now be written as[4]:

$$< \sigma v >= \iint dv_1 dv_2 \sigma_{1,2}(v) v f_1(v_1) \qquad \text{.....(2-31)}$$

Where $v = |v_1 - v_2|$ and the integrals are taken over the three-dimensional

velocity space. In order to put Eq(2.31) in a form suitable for integration, we express the velocities v_1 and v_2 by means of the relative velocity and of the center-of-mass velocity[4]:

$$v_c = (m_1 v_1 + m_2 v_2)/(m_1 + m_2) : \quad \text{.....(2-32)}$$

$$v_1 = v_c + v m_2/(m_1 + m_2) \quad \text{.....(2-33)}$$

$$v_2 = v_c - v m_1/(m_1 + m_2)$$

Equation 2.31 then becomes[4]:

$$< \sigma v >= \frac{(m_1 m_2)^{3/2}}{(2\pi k_B T)^3} \times \iint dv_1 dv_2 \exp(-\frac{(m_1+m_2){v_c}^2}{2k_B T} - \frac{m_r v^2}{2k_B T})\sigma(v)v \quad \text{....(2-34)}$$

Where m_r is the reduced mass defined by eqn 1.4, and the subscripts '1,2' have been omitted. It can be shown (see, for example, Clayton 1983) that the integral over $dv_1 dv_2$ can be replaced by an integral over $dv_c dv$, so that we can write[4]:

$$< \sigma v >= \left[(\frac{(m_1+m_2)}{2k_B T})^{3/2} \int dv_c \exp(-\frac{(m_1+m_2)}{2k_B T}{v_c}^2)\right] \times$$

$$(\frac{m_r}{2\pi k_B T})^{3/2} \int dv \exp\left(-\frac{m_r}{2k_B T}{v_c}^2\right) \sigma(v)v \quad \text{.....(2-35)}$$

The term in square brackets is unity, being the integral of a normalized Maxwellian, and we are left with the integral over the relative velocity. By writing the volume element in velocity space as $d\mathbf{v} = 4\pi v^2\, dv$, and using the definition 1.3 of center-of-mass energy ϵ, we finally obtained[4]:

$$< \sigma v > = \frac{4\pi}{(2\pi m_r)^{1/2}} \frac{1}{(k_B T)^{3/2}} \int_0^\infty \sigma(\epsilon)\epsilon \exp\left(-\frac{\epsilon}{k_B T}\right) d\epsilon \ldots\ldots (2\text{-}36)$$

Most modern computer simulations of fusion reaction rates utilize fitting functions based on reaction rates calculated from data that was published almost thirty years ago **[39]**. During the course of the last thirty years, improved experimental techniques were developed that allowed for the collection of more accurate data at low plasma temperatures [**40**].

For the above purpose we optimize of the new reaction rate model proposed by H. S. Bosch and G. M. Hale [**40**] and compares their R-matrix reaction rate model with the published values found in the Naval Research Laboratory (NRL) Plasma Formulary [**41**], the BUCKY 1-D radiation hydrodynamics code developed at the University of Wisconsin – Madison [**42**] and the DRACO 2-D radiation hydrodynamics code developed at the Laboratory for Laser Energetics (LLE) [**43**].

$$< \sigma v > = exp\left[\frac{A_1}{T^r} + A_2 + A_3 T + A_4 T^2 + A_5 T^3 + A_6 T^4\right]$$

The coefficients for this equation are given in the table (2.3)

Table(2.3) coefficients used in the reaction rate polynomial[44]

	$T(d,n)^4He$	DD_{total}	$^3He(D,p)^4He$
A_1	-2.1377692E+01	-1.5511891E+01	-2.7764468E+01
A_2	-2.5204050E+01	-3.5318711E+01	-3.1023898E+01
A_3	-7.1013427E-02	1.2904737E-02	2.7889999E-02
A_4	1.9375450E-04	2.6797766E-04	-5.5321633E-04
A_5	4.9246592E-06	-2.9198658E-06	3.0293927E-06
A_6	-3.9836572E-08	1.2748415E-08	-2.5233325E-08
r	0.2935	0.3735	0.3597

2.3.1 Gamow form for non-resonant reactions

Useful and enlightening analytical expressions of the reactivity can be obtained by using the simple parametrization in Eq(2.9) of the cross-section. In this case the integrand of Eq(2.36) becomes[4]:

$$y(\epsilon) = S(\epsilon)exp\left[-\left(\frac{\epsilon_G}{\epsilon}\right)^{1/2}\right] = S(\epsilon)g(\epsilon, k_BT) \qquad \text{.....(2-37)}$$

An interesting result is obtained for temperatures $T << \epsilon_G$ and stems from the fact that the function $g(\epsilon, k_BT)$ is the product of a decreasing exponential coming from the Maxwellian times an increasing one originating from the barrier penetrability, as shown in Fig. 2.3 It has a maximum at the Gamow peak energy**:**

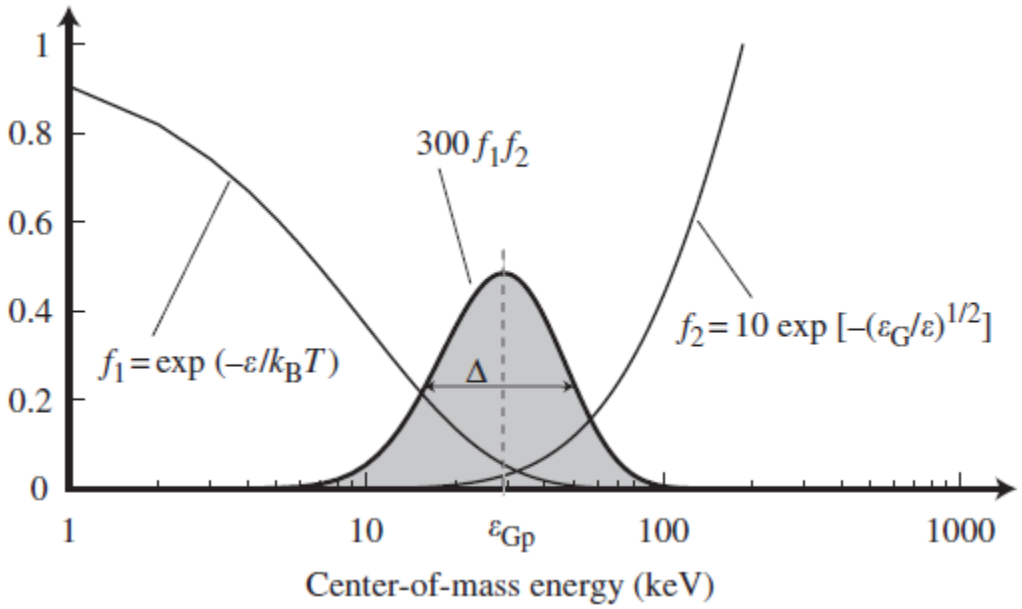

Fig. 2-3 Gamow peak for DD reactions at *T* = 10 keV: most of the reactivity comes from reaction between nuclei with center-of-mass energy between 15 and 60 keV[4].

From the barrier penetrability, as shown in Fig.2.3 It has a maximum at the Gamow peak energy[4]:

$$\epsilon_{G_P} = \left(\frac{\epsilon_G}{4k_B T}\right)^{1/3} k_B T = \xi k_B T \qquad \text{.....(2-38)}$$

where, for Eq(2.8)**:**

$$\xi = 6.2696(Z_1 Z_2)^{2/3} A_r{}^{1/3} T^{-1/3} \qquad \text{.....(2-39)}$$

with the temperature in kiloelectron Volt. To perform the integration we use the saddle-point method, that is, we first expand *y(ϵ)* in Taylor series around $\epsilon = \epsilon_{G_P}$, thus writing**:**

$$y(\epsilon) \cong S(\epsilon) exp\left[-3\xi + (\frac{\epsilon - \epsilon_{G_P}}{\Delta/2})^2\right] \quad \text{.....(2-40)}$$

with

$$\Delta = \frac{4}{\sqrt{3}}\ \xi^{1/2}\ k_B T \quad \text{.....(2-41)}$$

Equation 2.40 shows that most of the contribution to the reactivity comes from a relatively narrow energy region with width Δ centered around $\epsilon = \epsilon_{G_P}$, in the high energy portion of the velocity distribution function (see Fig. 2.3) Gamow peak .

Using eqns 2.37–2.41 and with the further assumption of nonexponential behaviour of *S(ϵ)* we can integrate eqn 2.35 to get the reaction rate in the so-called Gamow form[4]:

$$< \sigma v > = \frac{8\ \hbar}{\pi\ \sqrt{3}\ m_r\ Z_1 Z_2 e^2}\ \bar{S}\ \xi^2\ exp(-3\xi) \quad \text{.....(2-42)}$$

Here, we have used

$$\int_0^\infty exp(-x^2)dx = \sqrt{\pi}\ /2$$

and indicated with $\bar{S}$an appropriately averaged value of *S*. In the cases in which *S* depends weakly on ϵ, one can simply set $\overline{S}$ = *S(0)*. In the following, when distinguishing between $\bar{S}$ and *S(0)* is not essential, we shall simply use the symbol *S*. Improved approximations, taking into account the dependence of *S* on ϵ are discussed by Clayton (1983) and Bahcall (1966). Inserting the values of the numerical constants Eq(2.42) becomes:

$$< \sigma v > = \frac{6.4\times10^{-18}}{A_r Z_1 Z_2}\ S\ \xi^2\ exp(-3\xi)\ cm^3/s \qquad \text{.....(2-43)}$$

where *S* is in units of kiloelectron Volt barn and ξ is given by Eq(2.39). We remark that the Gamow form is appropriate for reactions which do not exhibit resonances in the relevant energy range. In particular, it is a good approximation for the DD reactivity, while it is not adequate for the DT and D ^3He reactions.

Equation 2.43 can be used to appreciate the low-temperature behaviour of the reactivity. By differentiation we obtained:

$$\frac{d<\sigma v>}{<\sigma v>} = -\frac{2}{3} + \xi\frac{dT}{T} \qquad \text{.....(2-44)}$$

Which leads to

$$< \sigma v > \propto T^{\xi} \qquad \text{.....(2-45)}$$

when

$$\xi \gg 1$$

A strong temperature dependence is then found when:

$$T \ll 6.27 {Z_1}^2 {Z_2}^2\ A_r$$

making apparent the existence of temperature thresholds for fusion , which are increasing functions of the mass of the participating nuclei.[4]

2.4 Suggestion models:

2.4.1 The model I:

In most of the literatures, resonant tunneling of the Coulomb barrier for the nuclear reaction was treated as a two-step process. That is: tunneling first; then, decay. The tunneling probability was calculated in an oversimplified one-dimensional model [**45]** , and the decay was assumed to be independent of the tunneling process. Nevertheless, this is not true in the case of the light nuclei fusion. In reality, when the wave function of the projectile penetrates the Coulomb barrier, it will reflect back and forth inside the nuclear well. This reflection inside the nuclear well is totally neglected in the one-dimensional model where the wave has no reflection as long as it penetrates through the barrier.(In the case of α-decay, the outgoing α-particle will have no reflection after penetrating the Coulomb barrier even if in 3-dimensional model [**46**]). Indeed this reflection is essential for the resonant penetration into the center of nuclear well through the Coulomb barrier. Secondary, the decay of the penetrating projectile will terminate the motion of bouncing back and forth inside the nuclear well. If nuclear reaction happens quickly; then, the wave function will have no time to bounce back and forth. That is: the short lifetime of the penetrating wave may not allow a resonant tunneling, because there will be no enough bounce motion to build-up the wave function in terms of constructive interference inside the nuclear well. In a word, the tunneling and the decay in the light nucleus fusion should be combined together as a selective process. Tunneling and decay are no longer independent.

It has been shown that an imaginary part of potential inside the nuclear well is a proper way to consider this lifetime effect on the resonant

tunneling. A complex nuclear potential is proposed to describe this resonant tunneling effect for sub-barrier fusion in a 3-dimensional model for wide range of the energy of the projectile[**47-49**] . In that 3-dimensional calculation, instead of conventional phase shift, δo , we introduced a new pair of parameters: W_r and W_i , the real and the imaginary parts of the cotangent of phase shift, i.e.[47]

$$cot\delta_\circ = W_r + iW_i \qquad \ldots\ldots\ldots(2\text{-}46)$$

Thus, the fusion cross section for S wave will have a simple expression as[48]:

$$\sigma_r{}^{(0)} = \frac{\pi \quad (-4W_i)}{k^2\, W_r{}^2 + (W_{i-1})^2} \qquad \ldots\ldots\ldots(2\text{-}47)$$

This equation (2.47) expresses the resonant feature without invoking any Taylor expansion. When W_r =0, the cross section reaches the resonance peak. On the other hand, W_i determines the height and width of the resonance peak. Hence, we may call W_r the resonance function, and W_i the damping function. W_r and W_i may be expressed as the function of two other parameters: U_{1r} and U_{1i}, i.e. the real and the imaginary parts of the nuclear Potential [49]

$$W_r = \theta^2 \left\{ \frac{a_c\, z_r \sin(2z_r) + z_i \sinh(2z_i)}{a\ 2[sin^2(z_r) + sinh^2(z_i)]} - 2\left[ln\left(\frac{2a}{a_c}\right) + 2C + \hbar(ka_c) \right] \right\} \ldots\ldots(2\text{-}48)$$

$$W_i = \theta^2 \left\{ \frac{a_c\, z_i \sin(2z_r) - z_r \sinh(2z_i)}{a\ 2[sin^2(z_r) + sinh^2(z_i)]} \right\} \qquad \ldots\ldots(2\text{-}49)$$

Here 1/ θ^2 is the famous Gamow penetration factor,

$$\theta^2 = \frac{1}{2\pi}\left[exp\left(\frac{2\pi}{k\ a_c}\right) - 1\right] \qquad \text{…….(2-50)}$$

It is a function of incident energy *E* only, because:

$k^2 = (2m_r/\hbar^2)E$, and $a_c = \hbar^2/(Z_1 Z_2 e^2 m_r)$

is a constant(the Coulomb unit of length). Here m_r is the reduced mass, Z_1 and Z_2 are the charge number for the colliding nuclei, respectively; e is the charge unit of electricity, ħ is the Planck constant divided by 2π. A complex number z is defined as[50]:

$$z = k_1 a \equiv k_{1r} a + i k_{1i} a \equiv z_r + i z_i \qquad \text{……..(2-51)}$$

$$k_1{}^2 = \left(\frac{2m_r}{\hbar^2}\right)(E - U_{1r} - iU_{1i}) \qquad \text{……..(2-52)}$$

k_1 is the wave number inside the nuclear well. *a* is the radius of the nuclear well:

$a = a_\circ(A_1{}^{1/3} + A_2{}^{1/3})$

$A_1$and A_2 are the mass number for the colliding nuclei, respectively. $a_\circ$=1.746 fm to give the correct diameter for deuteron (4.4 fm) [**50**]. C=0.577…is Euler constant. h($k\ a_c$) is related to the logarithmic derivative of Γ function[50]:

$$h(x) = \frac{1}{x^2}\sum_{n=1}^{\infty}\frac{1}{n(n^2+x^{-2})} - C + \ln(x) \qquad \text{……..(2-53)}$$

When this model was applied to the d+t fusion cross section near 100 keV, it was a surprise to see the good agreement between the theoretical calculation and data points from the evaluated nuclear data file (ENDF/B-VI). There are only two adjustable parameters, U_{1r} and U_{1i} , in this model. We may adjust them to meet the resonance peak (5.01 barns at 110 keV); then, it will reproduce the data points covering the range of energy from 200 eV to 500 keV. [**51**]:

$$\sigma = \frac{A_5 + \frac{A_2}{(A_4 - A_3 E)^2 + 1}}{E\left[\exp\left(\frac{A_1}{\sqrt{E}}\right) - 1\right.} \qquad \text{……..(2-54)}$$

Where the coefficients $A_1, A_2, A_3, A_4,$ and A_5 are called the Duane coefficients and are given in the table(2.3),E is the laboratory energy.

These empirical parameters are evaluated by nonlinear least-squares fitting to available measurement [**52**]:

Table 2.4 NRL Plasma Formulary 5-parameter list[27].

			D+D Fusion	
	D+T Fusion	D+ ^3He Fusion	p+T	n+ ^3He
A_1	45.95	89.27	46.097	47.88
A_2	50200	25900	372	482
A_3	1.368×10^{-2}	3.98×10^{-3}	4.36×10^{-4}	3.08×10^{-4}
A_4	1.076	1.297	1.220	1.177
A_5	409	647	0	0

2.4.2 The model II:

The Gamow cross section Eq. (2.57) is based on a calculation of the probability that an incident nucleus can tunnel quantum mechanically through the repulsive Coulomb barrier of another and so allow a nuclear reaction to occur. A simple approximate way to do the calculation is to use the one-dimensional Schrodinger equation where[53]:

$$\left[\frac{\hbar^2}{2m}\frac{\partial^2}{\partial x^2} + (E - V(x))\right]\psi = 0 \qquad \text{.....(2-55)}$$

where E is the total energy and the potential energy is taken as[53]

$$V(x) = \frac{e^2}{4\pi\epsilon_\circ x} \quad for\ x > 0$$

$$= 0 \qquad \text{for } x < 0$$

the probability of a particle, incident from $x = +\infty$, tunneling through this barrier is proportional to[53]:

$$exp - \left[\frac{e^2}{4\pi\epsilon_\circ x}\frac{\sqrt{2m}}{\hbar}\frac{\pi}{2E^{1/2}}\right] \qquad \text{.....(2-56)}$$

$$\sigma_n = \frac{71}{E_D}\exp\left(-\frac{44}{E_D{}^{1}/_{2}}\right) \qquad \text{.....(2-57)}$$

where E_D is the incident energy (in the laboratory frame) of a deuteron in keV colliding with a stationary target deuteron [a barn (b) is $10^{-28}m^2$]. The

form of this expression is that obtained from an approximate theoretical treatment, but with the coefficients modified slightly to fit experiment. Using this form, which has good theoretical justification, is expected to provide reasonable accuracy even extrapolated to lower energies than the experimental results[**53**].

2.4.3 The model III:

If the potential energy between two particles depends only on distance, the force field is called the **central force field** and is given as F = -(dU/dr)r/r. In the center of the mass system, angular momentum L = r x p is conserved. Since M is constant, r stays on a plane perpendicular to M. In the polar coordinates (r; ϕ), the Lagrangian is given as,**[54]**

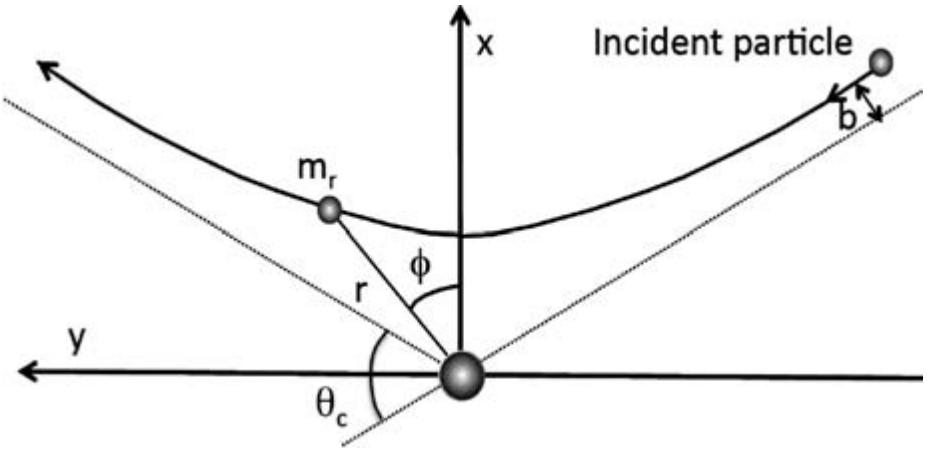

Figure (2.4) Particle orbit in Coulomb potential $r = \frac{r_\circ}{1-\alpha \cos\emptyset r_\circ} = \frac{b^2}{b_\circ}$, and $\alpha = (1 + (b/b_\circ)^2)^{1/2}$ [5]

$$L = m\left(\dot{r}^2 + r^2\dot{\emptyset}^2\right) - U(r) \qquad \text{.....(2-58)}$$

Since L is independent of ∅, canonical momentum conjugates to ϕ,

$$L = P_{\emptyset} = mr^2\dot{\emptyset}$$

is conserved. Substituting this relation into the energy conservation relation:

$$E = m\left(\dot{r}^2 + r^2\dot{\emptyset}^2\right) + U(r)$$

we obtain Eq(2.59)[54]

$$\frac{dr}{dt} = \sqrt{\frac{2\left(E-U(r)\right)}{m} - M^2/(m^2r^2)} \qquad \text{……..(2-59)}$$

In the case of repulsive Coulomb potential[54]:

$$U(r) = \frac{e_i e_j}{(4\pi\epsilon_\circ r)}$$

the particle orbit is given by following hyperbolic curve.

$$r = \frac{r_\circ}{1-\cos\emptyset} \qquad \text{…….(2-60)}$$

Where[54]

$$r_\circ = \frac{M^2}{m_r \frac{e_i e_j}{(4\pi\epsilon_\circ)}} \;, \alpha = \sqrt{1 + \frac{2EM^2}{(\frac{e_i e_j}{4\pi\epsilon_\circ})^2}} \qquad \text{…….(2-61)}$$

Since M = bm_r u and E = m_r u^2/2 (b is impact parameter in figure 2.4, u is particle speed at infinity), we can convert these parameters as follows:

$$r_\circ = \frac{b^2}{b_\circ} \quad , \quad \alpha = \sqrt{1 + \frac{b^2}{b_\circ{}^2}} \qquad \text{……..(2-62)}$$

Where:

$$b_\circ = \frac{e_i e_j}{4\pi\epsilon_\circ m_r u^2} \qquad \text{.....(2-63)}$$

The wave front of the incident wave should be perpendicular to this hyperbolic curve. Let k be the de Broglie wave number, the wave front satisfying this criteria is:

$$z + b_\circ \ln k(r - z) = const. \qquad \text{.....(2-64)}$$

where $b_\circ = \frac{e_i e_j}{4\pi\epsilon_\circ m_r u^2}$ =7.2 x 10^{-10} $Z_i Z_j / E_r$ (eV) (m), called the Landau parameter. The incident wave is already distorted at infinite distance before encountering the nucleus since the Coulomb field operates to infinity. So, the incident wave is given by :

$$exp[ik\{z + b_\circ \ln k(r - z)\}]$$

For a non-relativistic collision $E_r = p^2/2m_r = \hbar^2 k^2/2m_r$, and the Schrödinger's wave equation becomes:

$$[\partial^2/\partial x^2 + (k^2 - \beta/r)]\psi = 0$$

Where:

$$\beta = m_r e_i e_j / 2\pi\epsilon_\circ \hbar^2.$$

Substituting

$$\psi = \exp(ikz)F(x)$$

F should have the form:

F=F(r-z).

Then, the wave equation becomes:

$$\frac{\xi d^2F}{d\xi^2} + \frac{(1-ik\xi)dF}{d\xi} - \left(\frac{\beta}{2}\right)F = 0$$

For

$$\xi = r - z$$

Taylor expanding:

$$F(F = \sum_{n=0}^{\infty} a_n \xi^n (a_\circ = 1))$$

and substituting into the wave equation gives a_n and F is found to be the hyper geometric function F as follows,

$$\psi = \exp(-\pi\alpha/2)\Gamma(1+i\alpha)e^{ikz}F(-i\alpha, 1; ik\xi) \quad \text{.....(2-65)}$$

Here:

$$\alpha = \beta/2k \ , F(a,b;z) \equiv \sum \Gamma(a+n)\Gamma(b)z^n/\Gamma(a)/\Gamma(b)/\Gamma(n+1)$$

is a hypergeometric function, Γ is the gamma function. Permeability of the Coulomb barrier P is then given from wave function at the origin as,

$$P(E/E_C) = \frac{\sqrt{E_c/E}}{\exp(\sqrt{E_c/E})-1} \quad \text{.....(2-66)}$$

$$E_c = \frac{m_r e^4}{8\epsilon_\circ{}^2 \hbar^2} = 0.98A_r(MeV) \quad \text{.....(2-67)}$$

Here, m_r is the reduced mass .($m_a m_b/(m_a + m_b)$) between particles a and b, A_r is a mass number of the reduced mass, $\epsilon_\circ$ is the vacuum permittivity (= 8.854 x 10^{-12} F/m), and ħ is Planck's constant. Figure 2.5 shows permeability of the Coulomb barrier P against E/Ec. The critical energy Ec

given by equation (2.67). For the T(d,n)^4_2He reaction, it is 1.18MeV, while numerically fitting Ec to reproduce the measured fusion cross-section is 1.27MeV showing good agreement.

A particle with reduced mass jumping into the nuclear potential, will have higher kinetic energy than the original one (de Broglie wavelength shorter than the original de Broglie wavelength). Such big changes in wave number will cause a resonant interaction within the nucleus. For the DT fusion reaction, resonance energy and resonance width are E_r = 78.65 keV and Γ= 146 keV, respectively (figure 2.6) . The probability amplitude of a material wave is large since the compound nucleus ^5He has an energy level corresponding to a certain boundary condition.

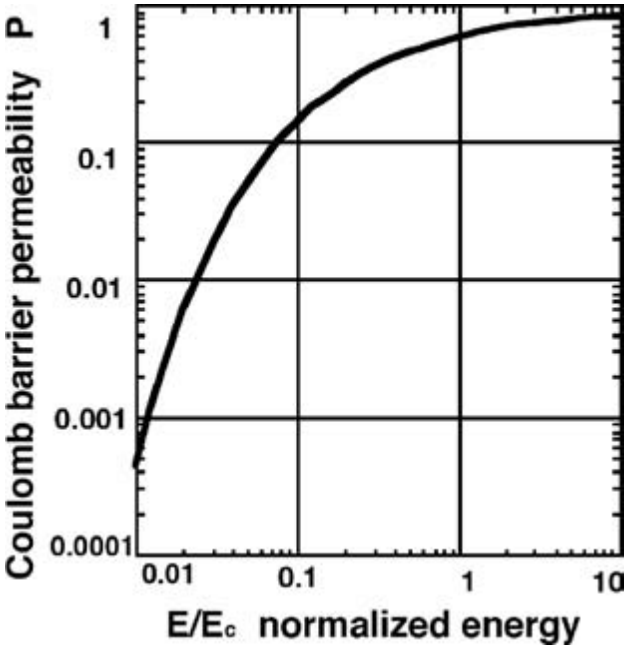

Figure (2.5) Energy dependence of the Coulomb barrier permeability. The Coulomb barrier permeability P is well-behaved (P → 1) in the high energy limit (E/Ec ≫ 1) while the formula given by Gamow P(E/Ec)=$(E/E_c)^{-1/2}$ exp$\left(-\left(\frac{E}{E_c}\right)^{-1/2}\right)$ [55] is valid only at low energy[5]

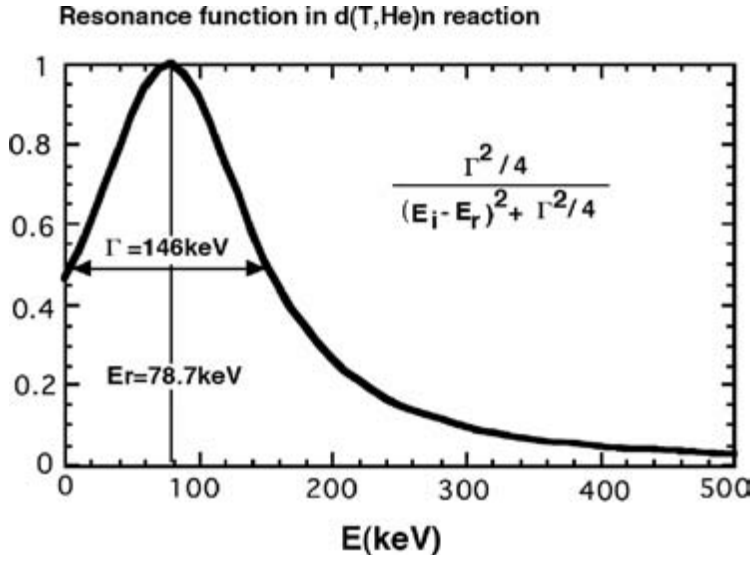

Figure (2.6)Normalized resonance function for DT reaction in laboratory frame[5]

The compound nucleus is unstable and will decay at a decay time constant. The decay time constant τ and the resonance width Γ have the relationship $\Gamma\tau = \hbar$, the decay time is calculated as τ= 4.5 x 10^{-21} s since Γ= 146 keV. This time is much longer (100 times) than the transit time of a nucleon with Fermi energy, τ_F=2R/v_F= 4.4 x 10^{-23}s. The fusion cross-section, considering the above, is given as,

$$\sigma_r = \pi\lambda\!\!\!^{-2} P(E/E_C)\frac{\Gamma_i\Gamma_f}{(E-E_r)^2+\Gamma^2/4} \qquad \text{.....(2-68)}$$

Here:

$$\lambda\!\!\!^{-2} = \hbar^2(2\mathrm{ME})^{-1}$$

and the second factor comes from the Breit–Wigner formula of resonance cross-section [**56**], here $\Gamma_i \sim k \sim 1/E^{0.5}$. In fact, the measured values of the fusion cross-section are given in a form of Equation 2.68 [**57**].

$$\sigma_r = \sigma_\circ \frac{E_{cl}}{E_l[exp\sqrt{E_{cl}/El}-1]}\left[\frac{1}{1+4(E_{l-}E_{rl})^2{\Gamma_l}^2}+\alpha\right] \qquad \text{.....(2-69)}$$

Here, $\sigma_\circ$= 23.79 b, E_{cl} =2.11MeV, E_{rl} = 78.65 keV, Γ_l = 146 keV,
α= 0.0081 for the T(d,n) ^4_2He reaction [**56**].

of nuclear fusion reactions (in the laboratory system) illustrating the dependence on deuterium energy. Deuterium energy in the laboratory frame E_l is related to the energy in the center of mass frame E as E= $m_t/(m_d+m_t)E_l$ and thus E_c=0.6E_{cl} = 1.27MeV.

Recently Li et al [**58**] gave more clear analysis of fusion cross section. Using the Landau's analysis of resonant scattering of charged particles [**56**], they derived different form of fusion cross section using the optical potential =$(U_r + iU_i)$ for D + T reaction as follows:

$$\sigma_r = \frac{\pi}{k^2\theta^2}\frac{-4w_i}{{w_r}^2+(w_i-\theta^{-2})^2} \qquad \text{.....(2-70)}$$

Where:

$$\theta^2 = (\exp\left((E_c/E)^{1/2}\right) - 1)/2\pi$$

and $w = w_r + iw_i = \cot(\delta_\circ)/\theta^2$

Where $\delta_\circ$ is phase shift due to nuclear potential. Using approximate expression:

w =C_1+C_2E_l+iC_3, fusion cross-section in laboratory frame is given as follows,

$$\sigma_r = \frac{-4\pi\ \hbar^2 \quad C_3}{2m_d\ E_l\theta^2{(C_1+C_2E_l)}^2+(C_4-\theta^{-2})^2} \qquad \text{.....(2-71)}$$

For DT fusion, C1 =- 0.5405, C2 = - 0.005546, C3 = -0.3909 gives good agreement with measured fusion cross-section[**5**]

Chapter Three

Calculations and Results

In this work we are using MATLAB program (version R2009a) to obtain on theoretical and experimental relations to calculate the fusion cross section that it is depend on quantum mechanics principle. And the results depends on three models to obtained and comparison with another results for fusion reaction.

The three models are described as follows:

3.1 model I:

The physics principle of this model is based on resonant tunneling effect of the Coulomb barrier for the nuclear reaction.(eq .2.54):

$$\sigma = \frac{A_5 + \sqrt{(A_4}}{E[\exp$$

Where the Coefficients A_1, A_2, A_3, A_4, A_5 are called the Duane coefficients and are given in the table(2-4)[26],E is the laboratory energy.

These empirical parameters are evaluated by nonlinear least-squares fitting to available measurement **[59]**.

In this research we calculate the cross section for nuclear fusion reactions for hydrogen isotopes with having applied usage extensive in production energy field as explained:

$D + T \rightarrow \alpha + n + 17.59$ MeV

$D + D \rightarrow T + P + 4.04$ MeV

$D + D \rightarrow {}^{3}_{2}He + n + 3.27$ MeV

$D + {}^{3}_{2}He \rightarrow \alpha + P + 18.35$ MeV

The calculations which are concerning cross sections for DD reaction is explained in the following figure(3-1)

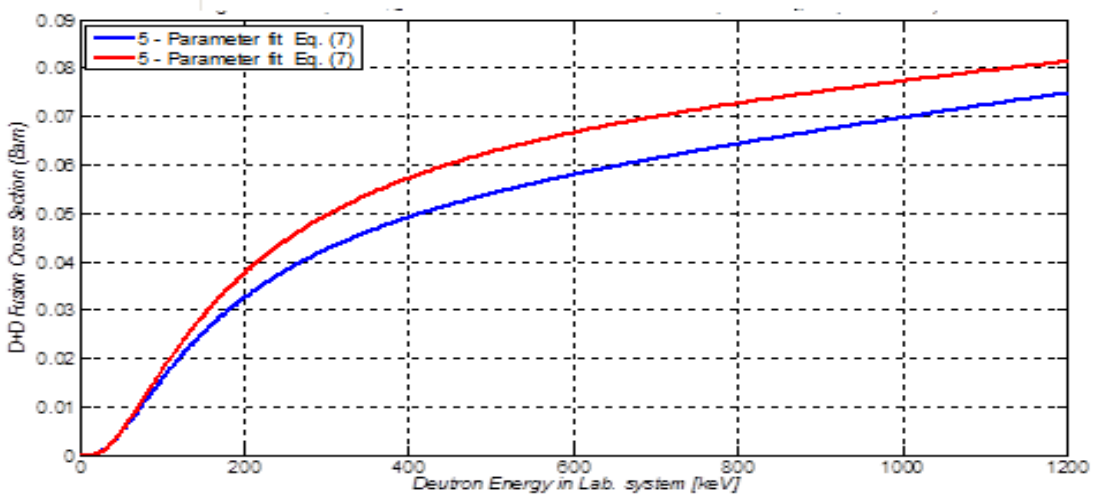

Figure(3.1) The Total fusion reaction cross section versus deuteron energy for D-D reaction.

The range of energy is between(10-1200 keV)

The calculations which are concerning cross sections for DT reaction is explained in the following figure (3-2)

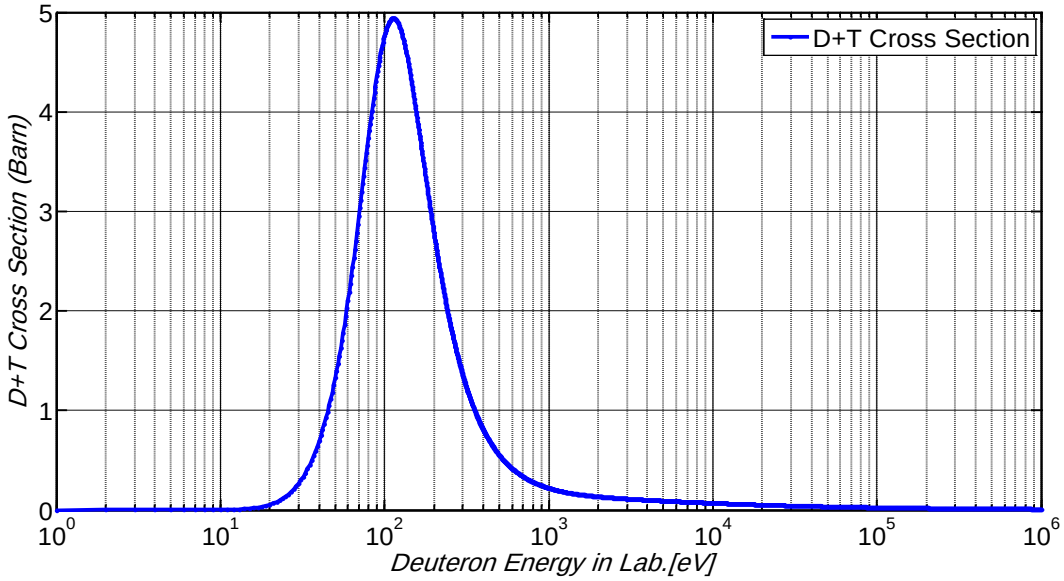

Figure(3.2) The Total fusion reaction cross section versus deuteron energy for D-T reaction

The range of energy is between (1-1000000 eV)

The calculations which are concerning cross sections for D ^3_2He reaction is explained in the following figure (3-3)

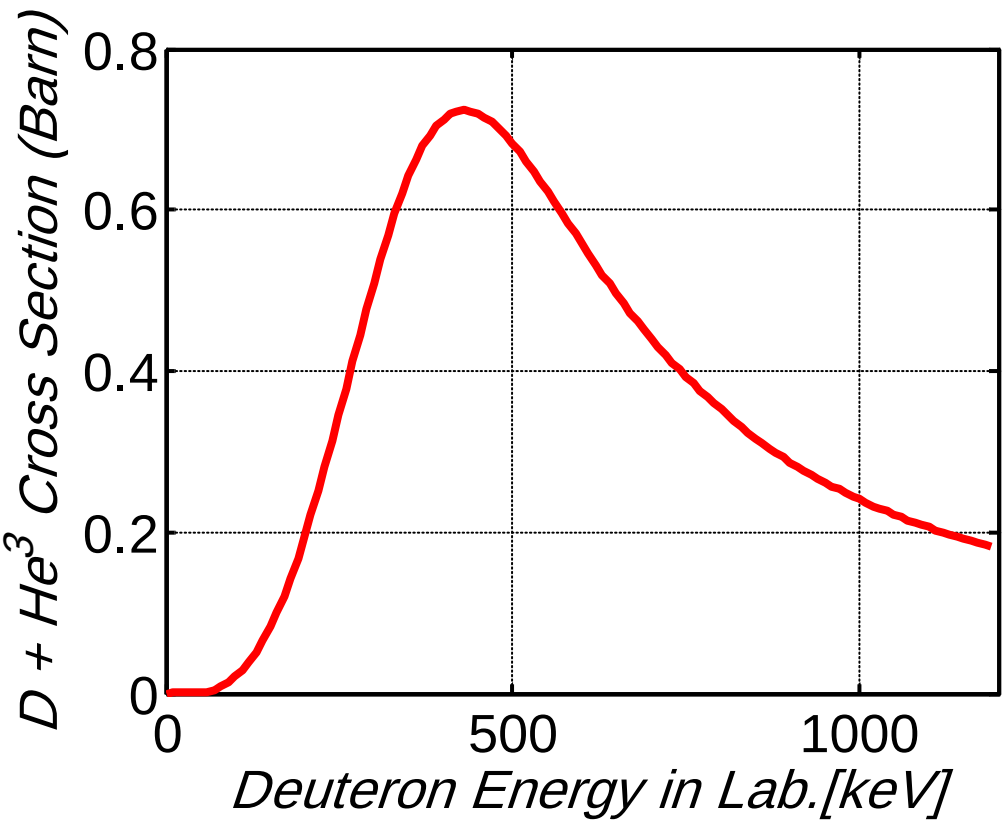

Figure(3.3) The Total fusion reaction cross section versus deuteron energy for D+$^{3}_{2}He$ reaction

The range of energy is between (10-1200 keV)

3.2 Model II :

The principle of physics for this model is based on repulsive Coulomb barrier of another and so allow a nuclear reaction to occur Eq(2.57)

$$\sigma_n = \frac{71}{E_D} \exp\left(-\frac{44}{E_D{}^{1}/_{2}}\right)$$

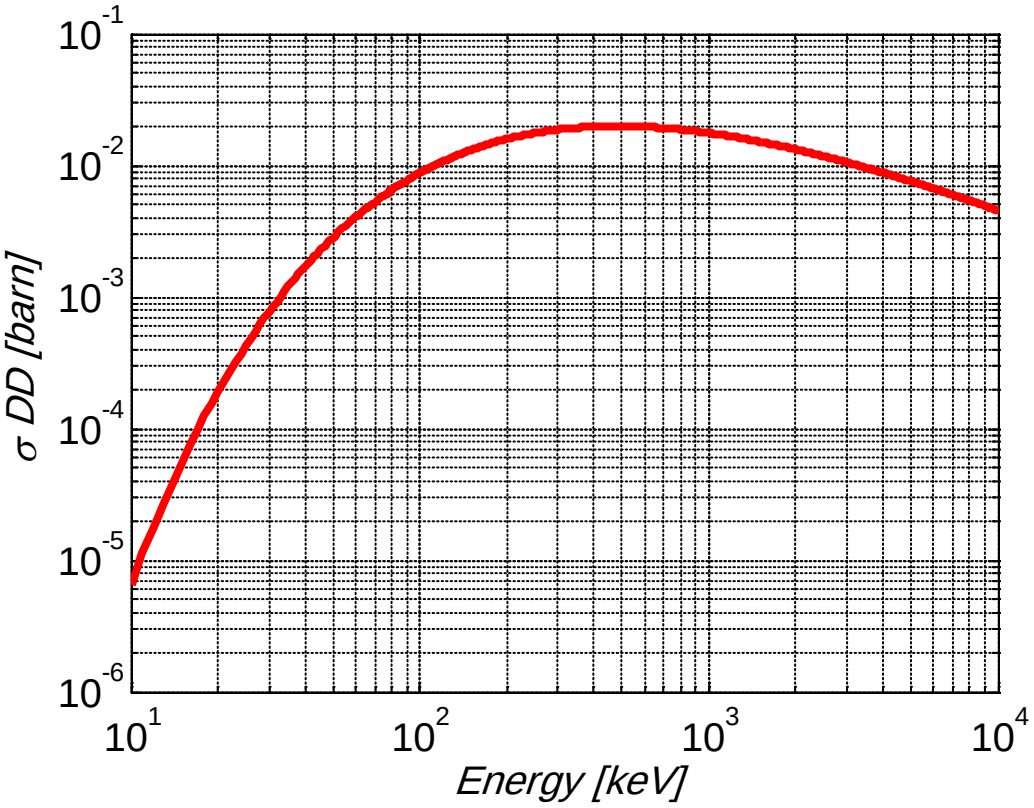

Figure(3.4) The Total fusion reaction cross section versus deuteron energy for D-D reaction

The range of the energy is between (10-10000 keV)

and we are calculate the reactivity for this reaction by using the following formula:[**53**]

$$\langle \sigma_n v \rangle = \frac{3.5 \times 10^{-20}}{T_D{}^{2/3}} \exp\left(-\frac{20.1}{T_D{}^{1/3}}\right) cm^3\ s^{-1} \quad \text{.....(3-1)}$$

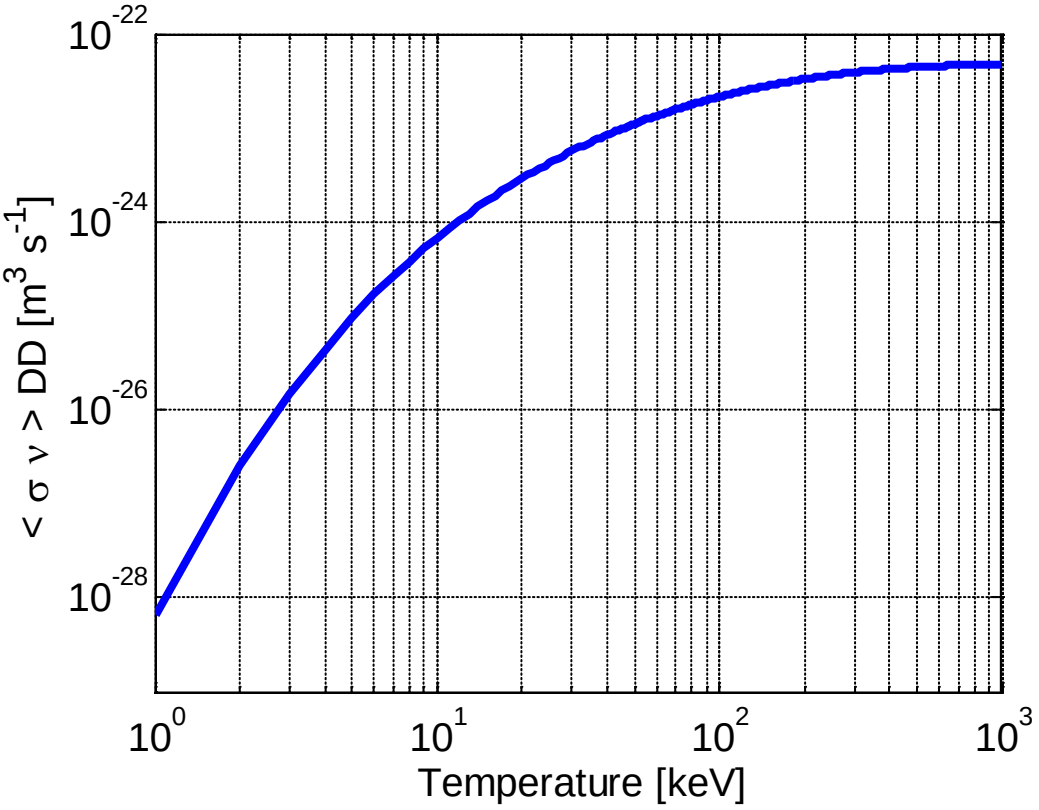

Figure(3.5) The D-D Reactivity versus deuteron temperature for D-D reaction.

The range of temperature is between (1 – 1000 keV)

3.3The model III:

The physics principle of this model is based on Coulomb scattering (E,q. 2.69)

$$\sigma_r = \sigma_\circ \frac{E_{cl}}{E_l[exp\sqrt{E_{cl}/El}-1]} \left[\frac{1}{1+4(E_{l-}E_{rl})^2{\Gamma_l}^2} + \alpha \right]$$

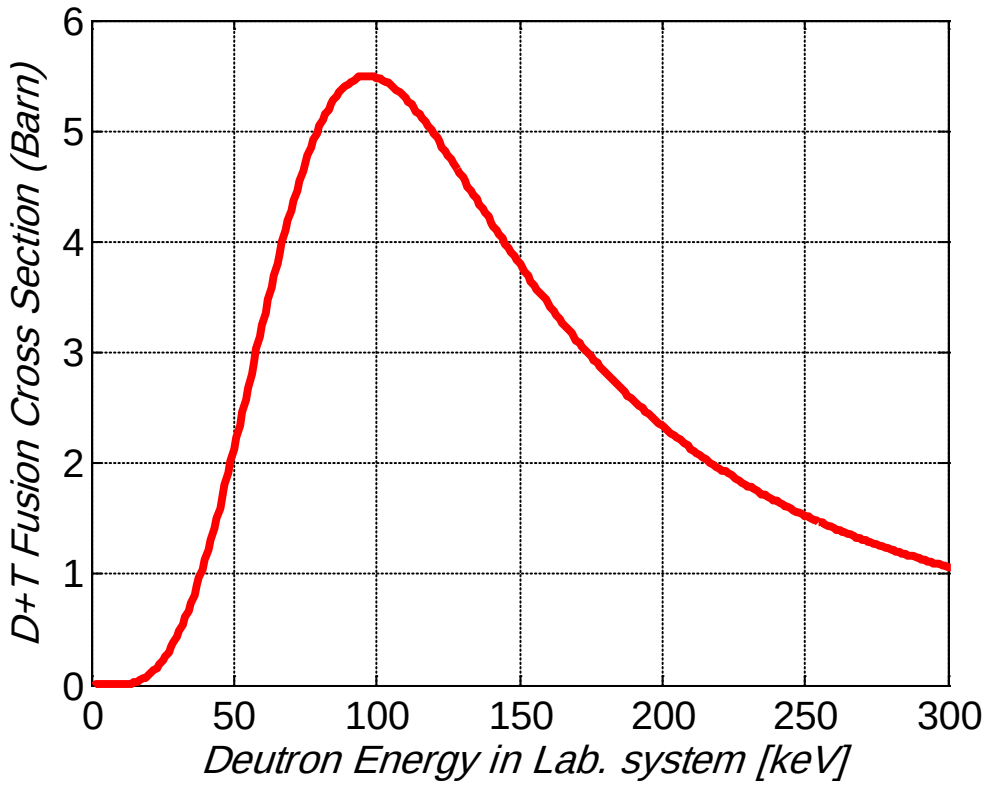

Figure(3.6) The Total fusion reaction cross section versus deuteron energy for D-T reaction

The range of energy is between (10 – 300 keV)

The equation (2.71)

$$\sigma_r = \frac{\pi \hbar^2 \quad -4C_3}{2m_{d\,E_l}\,\theta^2(C_1+C_2E_{l)}{}^2+(C_4-\theta^{-2})^2}$$

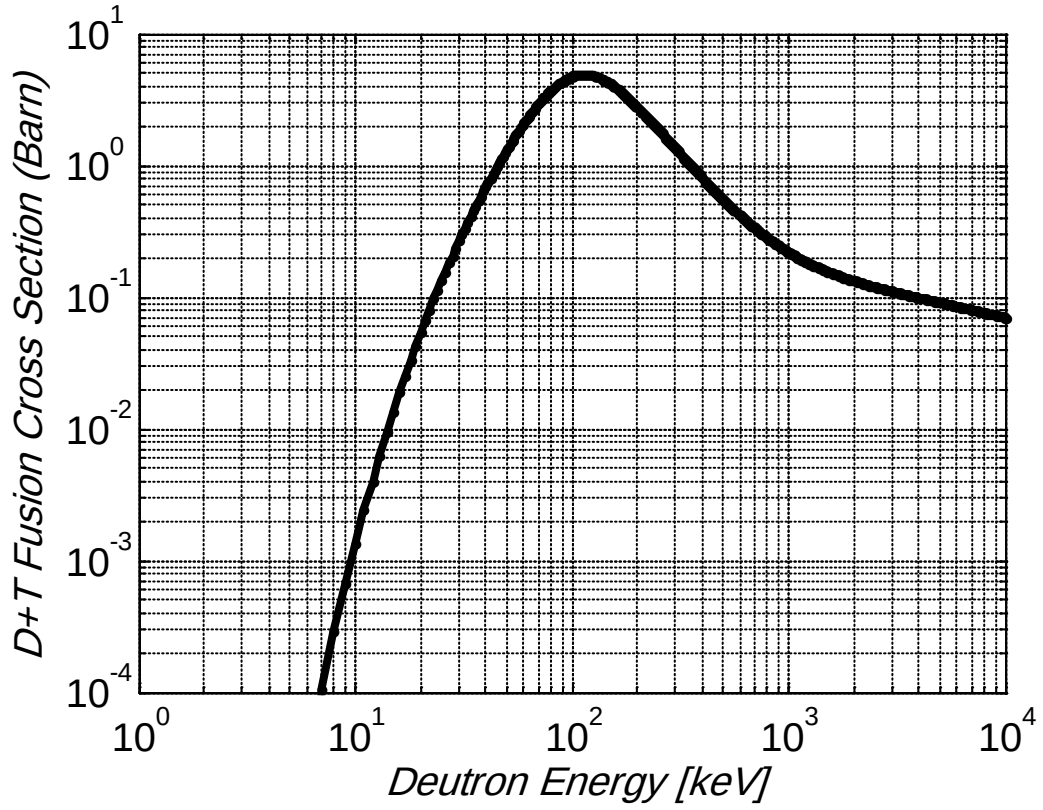

Figure(3.7) The Total fusion reaction cross section versus deuteron energy for D-T reaction.

The range of energy is between (10 – 10000 keV)

We are calculated the reactivity for D $^{3}_{2}He$ reaction by the equation:[**7**]

$$< \sigma v >_{D\ ^{3}He} = 4.98 \times 10^{-16} \exp\left(-0.152\left[ln\frac{T}{802.6}\right]^{2.65}\right)\ cm^3/s \quad \text{.....(3-2)}$$

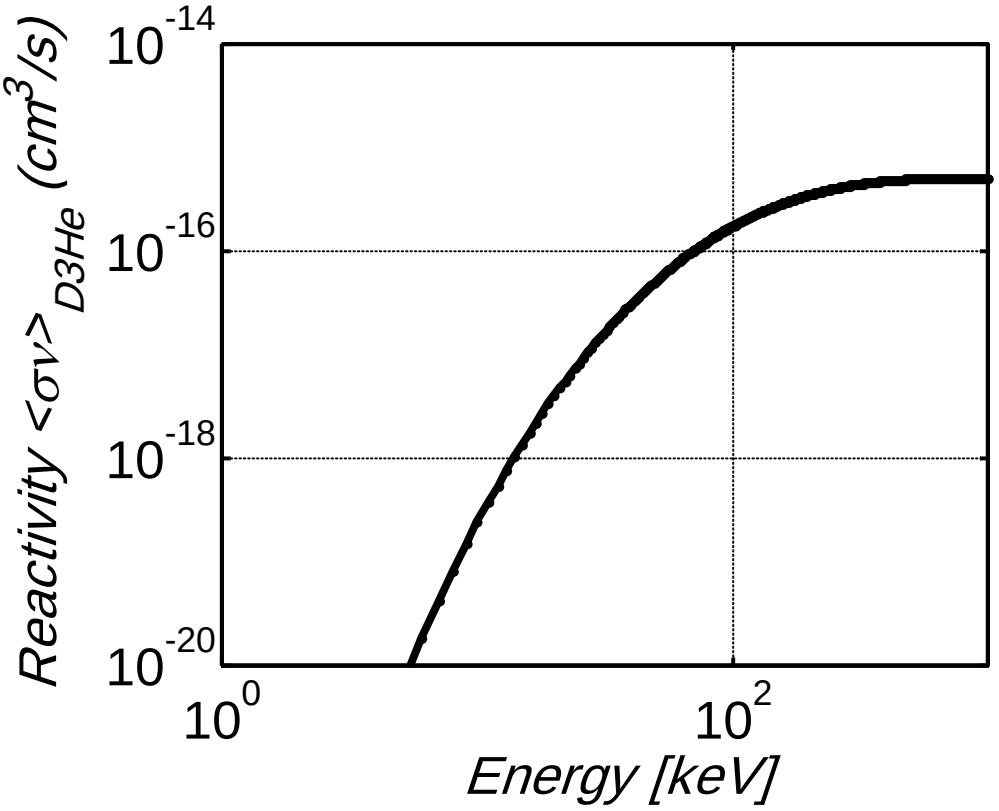

Figure(3.8) The D ^3_2He Reactivity versus deuteron temperature for D ^3_2He reaction.

The range of energy is between (10 – 150 keV)

And we are calculated the reactivity for D Dn reaction by using the following equation:[**7**]

$$< \sigma v >_{DD_n} = 2.27\times\ 10^{-14}\ \ \frac{1+0.00539T^{0.917}}{T^{2/3}} \exp\left(-\frac{19.80}{T^{1/3}}\right)\ cm^3/s \ldots (3\text{-}3)$$

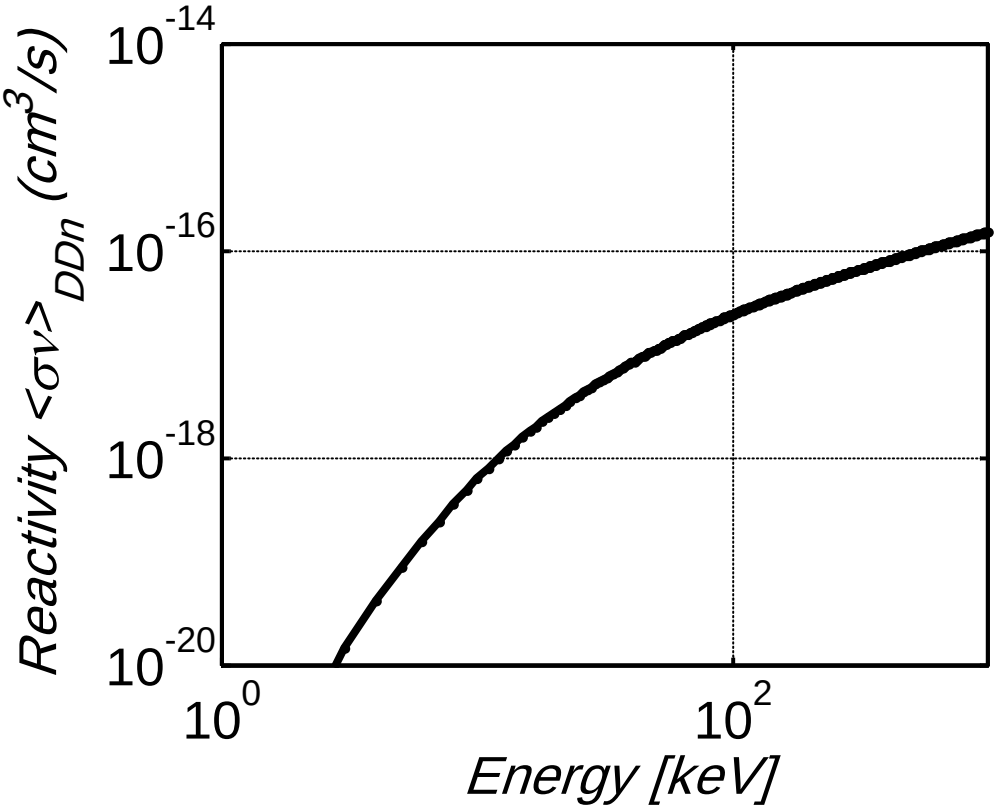

Figure(3.9) The D Dn Reactivity versus deuteron temperature for D Dn reaction.

The range of energy is between (10 – 150 keV)

And then calculated of reactivity for D Dp reaction by using the following equation:[7]

$$< \sigma v >_{DD_p} = 2 \times 10^{-14} \frac{1+0.00577 T^{0.949}}{T^{2/3}} \exp(-\frac{19.31}{T^{1/3}}) \ cm^3/s \ldots (3\text{-}4)$$

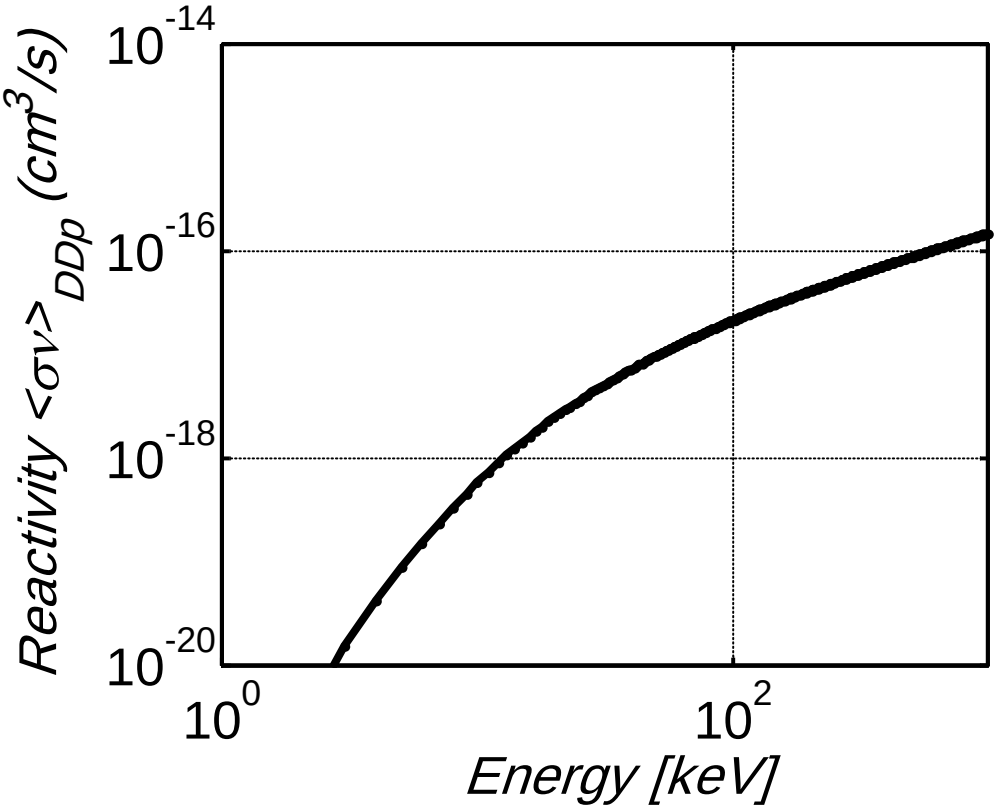

Figure(3.10) The D Dp Reactivity versus deuteron temperature for D Dp reaction.

The range of energy is between (10 – 150 keV)

And then calculated of reactivity for D T reaction by using the following equation:[7]

$$< \sigma v >_{DT} = 9.10 \times 10^{-16} \exp\left(-0.572\left[ln\frac{T}{64.2}\right]^{2.13}\right)\ cm^3/s \quad \ldots(3\text{-}5)$$

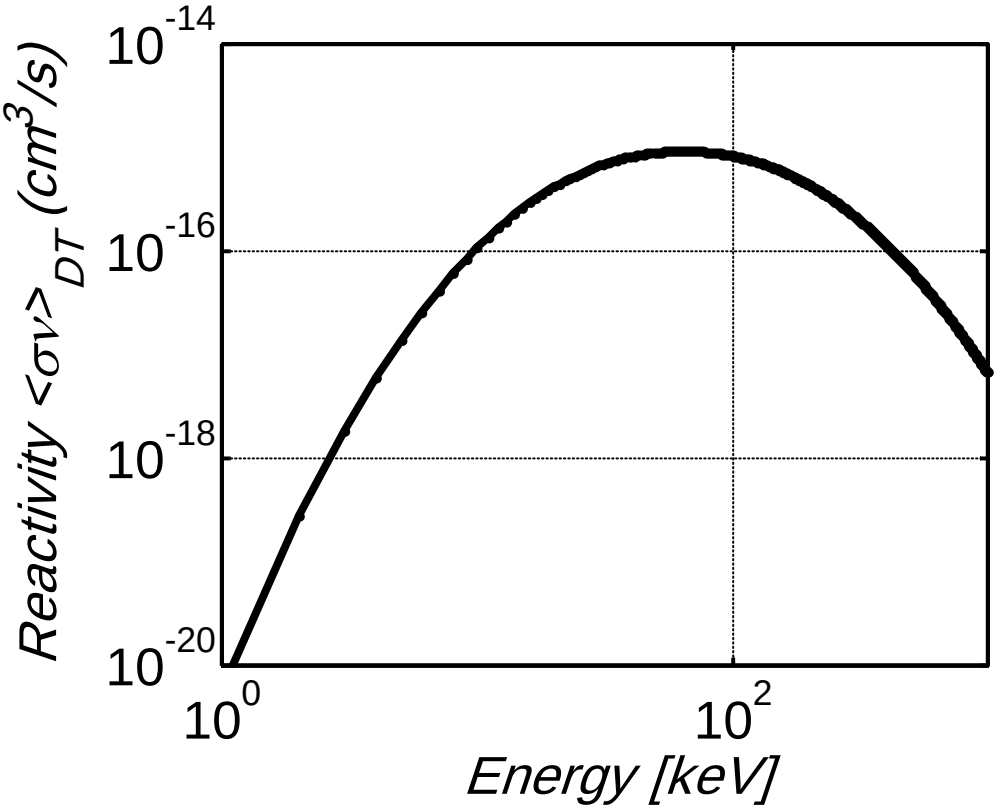

Figure(3.11) The D T Reactivity versus deuteron temperature for D T reaction.

The range of energy is between (1 – 150 keV)

And we are calculated the reactivity for P P reaction by using the following equation:[7]

$< \sigma v >_{PP}$ =1.56 × 10^{-37} $T^{-2/3}$ exp (-$\frac{14.94}{T^{1/3}}$)×(1+0.044T+2.03× $10^{-4}T^2$ +5× $10^{-7}T^3$) cm^3/s ……(3-6)

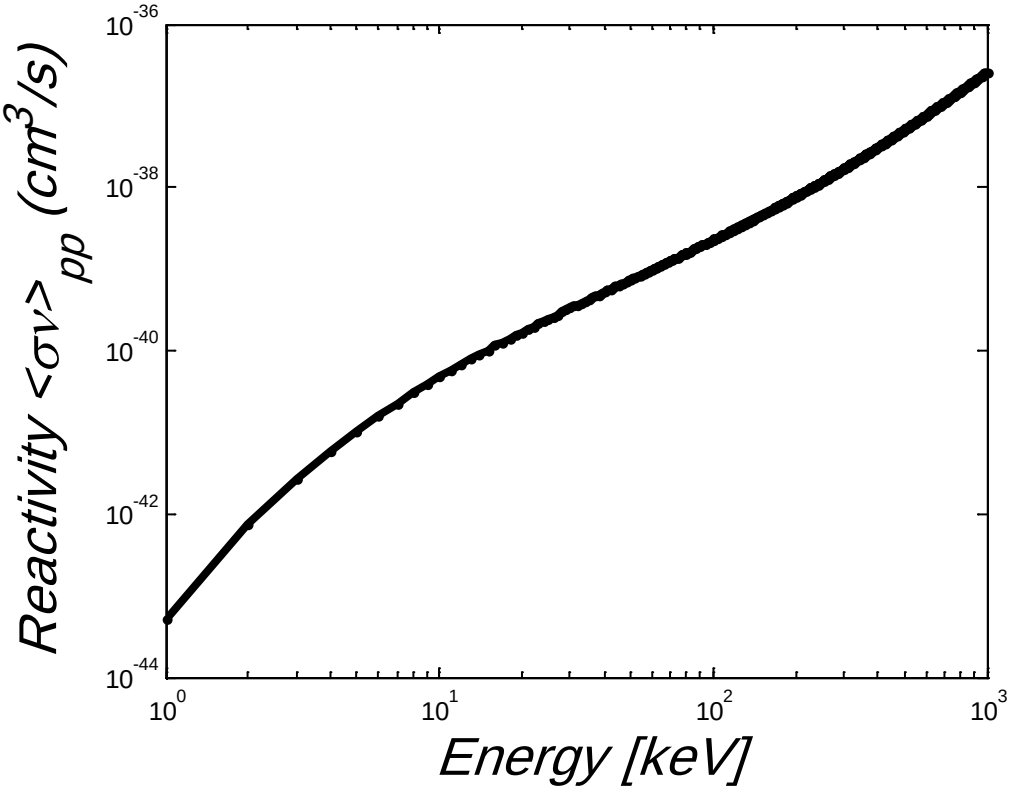

Figure(3.12) The p p Reactivity versus deuteron temperature for p p reaction.

The range of energy is between (1 – 1000 keV)

And also we are calculated the plasma power density for D D reaction by using the following formula:[**60**]

$P_{DD} = 3.3 \times 10^{-13} n_D{}^2 < \sigma v >_{DD}$ watt cm^{-3} ……(3-7)

Where n_D represents the deuterium density

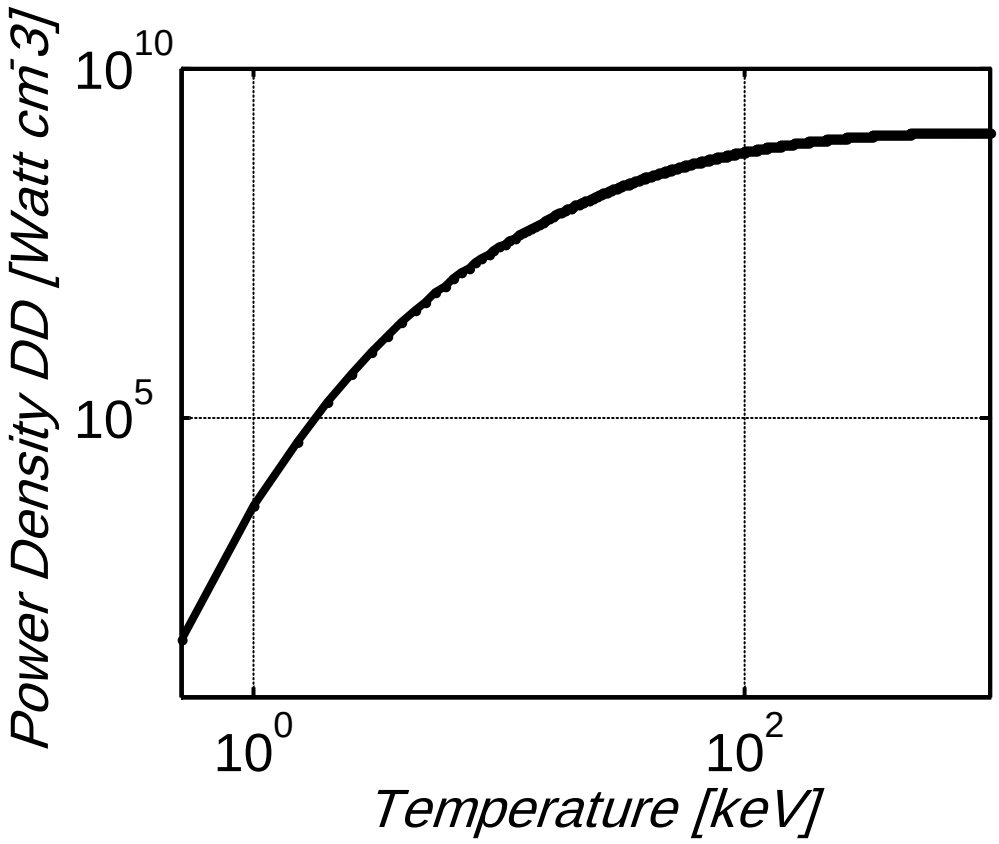

Figure(3.13) the plasma power density for D D reaction

The range of temperature is between (1 – 150 keV)

And also we are calculated the plasma power density for D T reaction by using the following formula**:[60]**

$P_{DT} = 5.6 \times 10^{-13} n_D n_T < \sigma v >_{DT}$ watt cm^{-3}……(3-8)

Where n_D, n_T are represent the deuterium density and tritium density respectively

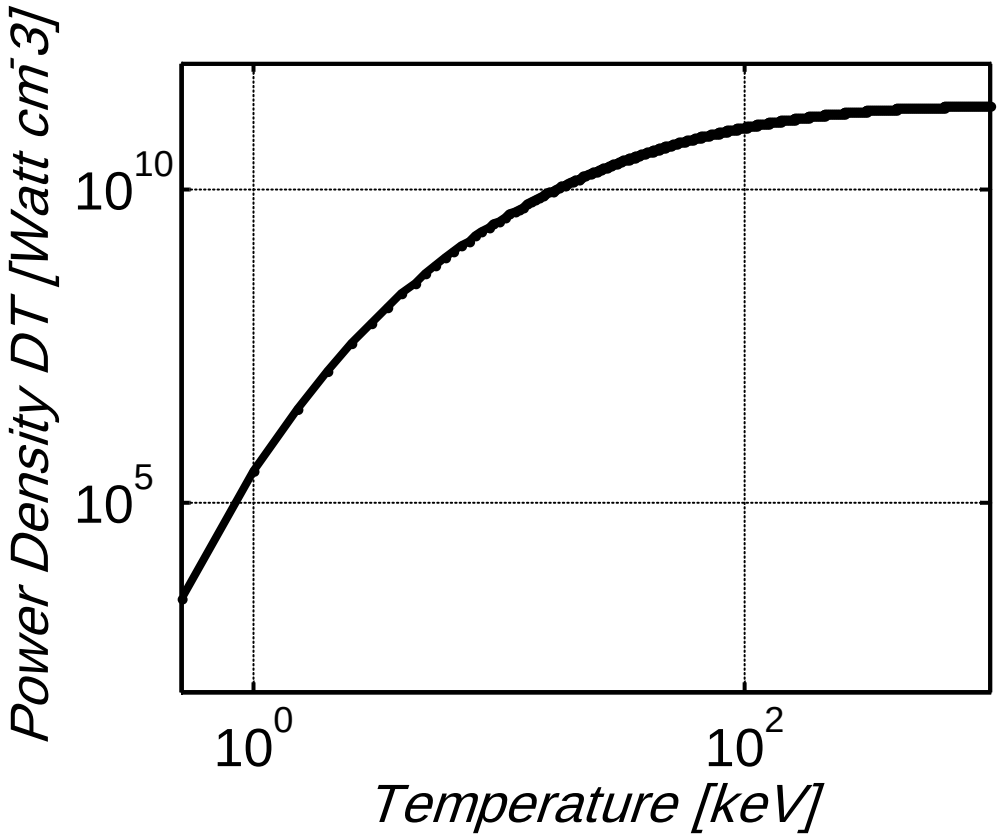

Figure(3.14) the plasma power density for D T reaction

The range of temperature is between (1 – 150 keV)

Chapter four

Discussion and Conclusion

The calculated results concerning fusion cross section for the reactions of hydrogen isotopes compared with the standard empirical as the results that shown in figure (4.1)

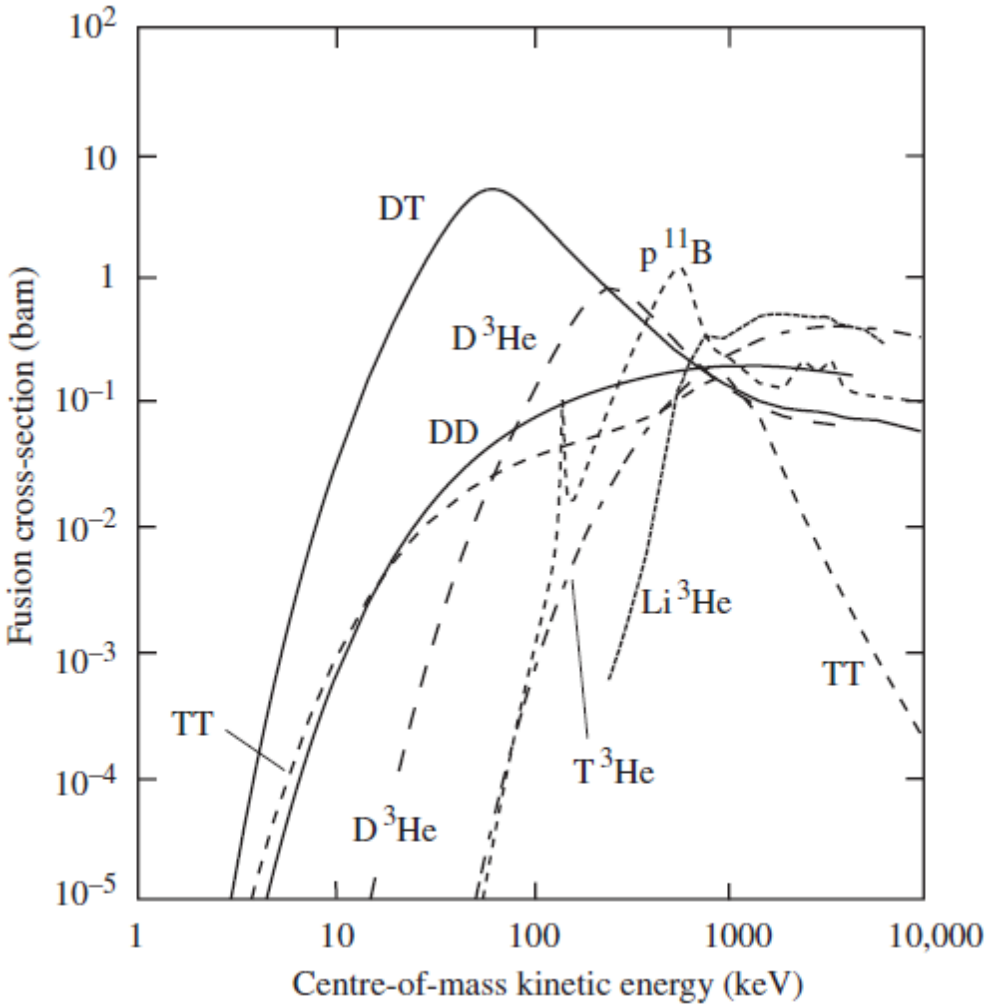

Figure(4.1)Fusion cross sections versus centre-of-mass energy for reactions of interest to controlled fusion energy [61].

In model I for the DD fusion reaction reveals an agreement with the standard experimental results that refer to the acceptability of calculations that explained by equation (2.54) and completely described in figure (3.1) .

And for the DT reaction we observe good agreement with the standard experimental results that refer to the acceptability of calculations relations used figure (3.2) .

And for the D $^{3}_{2}He$ reaction reveals a high agreement with the standard experimental results figure (3.3) .

In model III for the DT fusion reaction reveals an high agreement with the standard experimental results that refer to the acceptability of calculations that explained by equation (2.69) and completely described in figure (3.6) .

The calculated results concerning fusion cross section for the reactions of hydrogen isotopes compared with the standard empirical results are shown in figure (4.2).

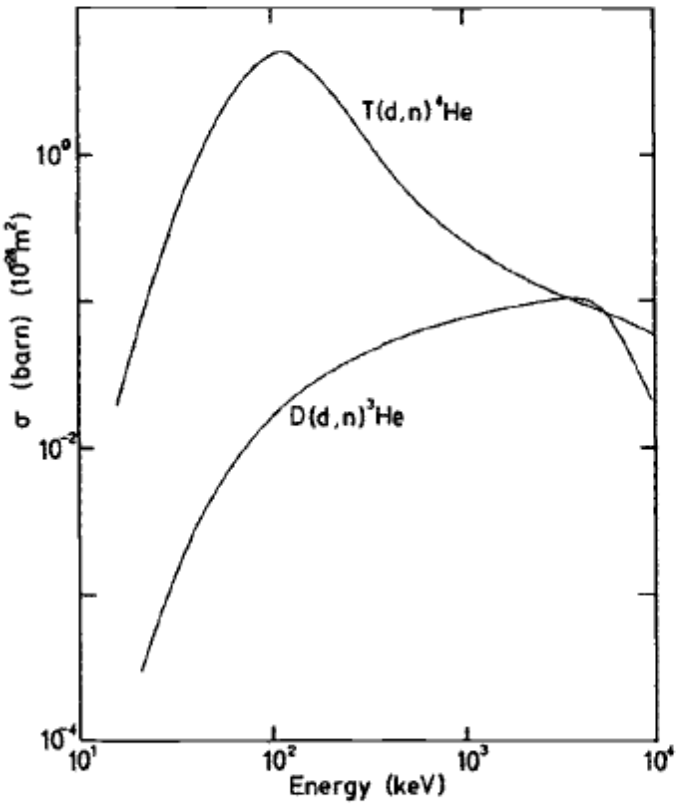

Figure (4.2) Neutron-producing fusion reaction cross sections (stationary target)[53].

In model II for the DD fusion reaction reveals an agreement with the standard experimental results that reflecting the acceptability of calculations that explained by equation (2.57) and completely described in figure (3.4).

From the observations above it can be concluded that the relations used in calculation the fusion cross section leading to the fact that contains most of the real physical phenomena that occur through interaction and this in turn leads to tranquility and admissibility in using these relations in the next calculations relating to the global physical factors influencing the design the devices and systems that depends on nuclear fusion technology such as reactivity, reaction rate, power released, fusion products, etc.

We conclude that the calculation of the controlled fusion cross sections plays a key role, notify can be considered as the important starting point in the design and completion of any design calculation programs or

practicability system or experiment because it can not be conclusion any of the influencing factors without the need to the fusion cross section of reaction and whenever it is accessed to experimental or theoretical relationship reflect a very high correspond increases of tranquility in entering into the construction of such systems especially those that are used for produce the power and hence the results related to the calculation the reactivity, reaction rate and power depends mainly on the fusion cross section.

Compare the results related to reactivity show in figures (3.8 - 3.12) with the international results published that shown in figure (4.3)

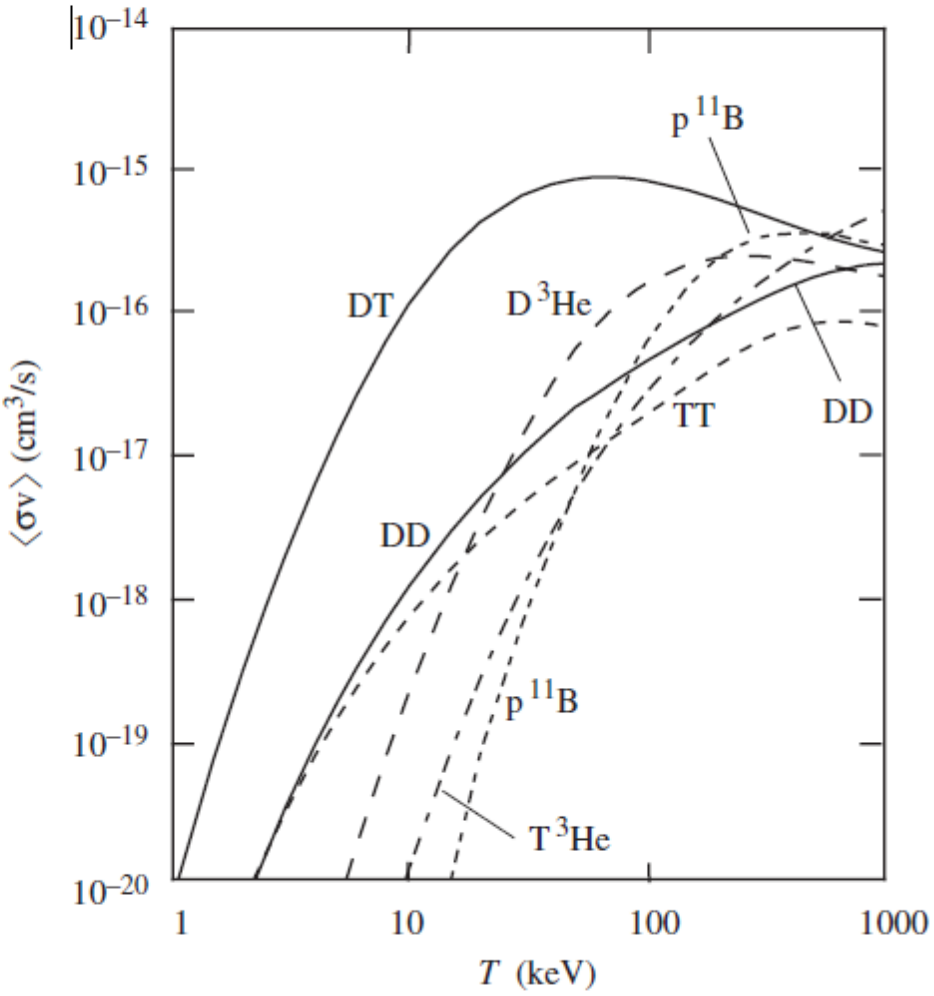

figure(4.3) Maxwell-averaged reaction reactivity versus temperature for reactions of interest to controlled fusion[4].

These figures reflect a high agreement and this in turn leads to a success in the calculations concern to the released power by its dependence on reactivity as shown in equations(3-7 and 3-8)

In figures (3.13 – 3.14) which describe the physical behavior for the power density output released by any systems that operated by the using of the hydrogen isotopes as a standard fuels gives or reflect a wide compatibility or agreement with the standard power density behaviors that shown in figure (4.4).

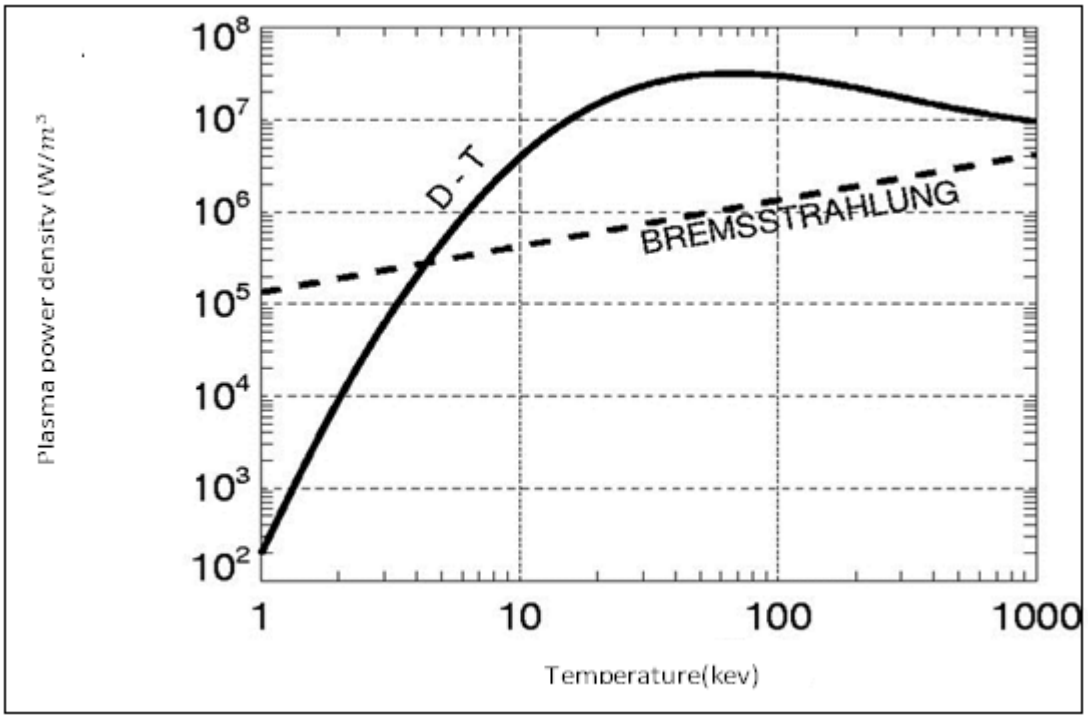

Figure(4-4):Variation of the D-T plasma power density with the incident deuteron temperature[60].

Conclusion:

Finally we obtained to a conclusion that if anyone interest in building or constructing a fusion system and they can really depend on the describing models in calculating the global fusion parameters and this fact are clearly observed by the our calculations or describing figures.

Future work

1. Extending the current study to include all controlled thermonuclear fusion reactions for the purpose of being acquainted with the status of each reactions in terms of identifying the priorities of its applications.

2. Preparation computer simulation model includes all fusion reactions as well as classical and quantum consideration.

3 .Studying the reactions known as Super Thermal and identifying areas of its applications preceded by the perception of the theoretical side relating to it.

4 . Studying the high life time for the heavy nucleus.

References

1. M. Keilhacker, A. Gibson, C. Gormezano and P.H. Rebut, “The Scientific Success of JET”, Nuclear Fusion, Volume 41, Number 12, 2001, pp. 1925-1935.

2. JT-60 Team, “Review of JT-60U Experimental Results in 1998”, JAERI 99-048.

3. Jordan E. Merelli, "Plasma position control in the Stor – M Tokamak" P.1 January, 2003 .

4. Engida H. Selato, "Nuclear Fusion Energy" Addis Ababa University, P.3, Julay, 2010.

5. M. Kikuchi, "Hydrogen Fusion: Light Nuclei and Theory of Fusion Reactions" Springer, P.15, 2011.

6. Asimov I Atom. Nightfall Inc. (1991)

7. Atzeni. "Nuclear Fusion Reactions" Chap.1, P.3, 2004.

8. J. M. Blatt, V. F. Weisskopf:" Theoretical Nuclear Physics", Chapter VIII, Springer-Verlag, 1979

9. Akito T. , Norio Y. "Fusion Rates of Bosonized Condensates", Osaka Univercity, Sept. 2006.

10. A. Takahshi, et al: JJAP, 41(2001)pp.7031-7046

11. M. Ohta, A. Takahashi: JJAP, 42(2002)pp.645-649

12. A. Takahashi:" Theoretical backgrounds for transmutation reactions", ppt slides for Sunday School of ICCF10, see http://www.lenr-canr.org/ Special Collection for ICCF10.

13. B. Povh, K. Rith, C. Scholtz, F. Zetsche: Teilchen und Kerne, Springer, 1994.

14. K. Yagi: Nuclear Physics (in Japanese), Asakura, Tokyo, 1971

15. L. I. "Schiff:Quantum Mechanics", McGraw-Hill (1955)

16. P. M. Morse, H. Feshbach; "Methods of Theoretical Physics", McGraw-Hill (1953)

17. X. Z. Li, et al: Phys. Rev. C, 61(2000)24610

18. Xing Z. Li , "Nuclear Physics for Nuclear Fusion ", The Journal of American Society, Vol. 41, No. 63, 2002.

19. Igor D. Kaganovich, Edward A. Startsev, et al, "Scaling Cross Section for Ion – Atom Impact Ionization" Prenceton University, Vol. 11, No. 3, November, 2003.

20. V. I. Zagrebaev* and V. V. Samarin, " Near – Barrier Fusion of Heavy Nuclei : Coupling of Channels", Joint Institute for Nuclear Research, Vol. 67, No. 8, November, 2003.

21. M. Yu. Romanovsky and W. Ebeling, " Fluctuations of Electric Microfields in Laser – Produced Ion Clusters : Enhancement of Nuclear Fusion", Humboldt University Berlen, Vol. 14, No. 6, June, 2003.

22. Xing Z. Li, Bin l., et al, " Fusion Cross Section for Inertial Fusion Energy ", Cambridge University Press, July, 2004.

23. L.F. Canto, R. Donangelo, et al, " Semiclassical Treatment of Fusion Processes in Collision of Weakly Bound Nuclei ", Institute de Fisica, 2005.

24. L.F. Canto, R. Donangelo, et al, " Theory of Breakup and Fusion of Weakly Bound Nuclei ", Institute de Fisica, 2005.

25. Ruggero M. Santilli, " Controlled Intermediate Nuclear ", Institute for Basic Research ", 2008.

26. Mark D., " Inertial Electrostatic Confinement Fusion Provides A potential Break Through in Designing and Implementing Practical Fusion Power Plants ", www.askamr.com , 2008.

27. Xing Z. Li, Qing M. Wei ,et al, " A new Simple Formula for Fusion Cross Section Light Nuclei ", Tsinghua University, October, 2008.

28. Yeong E. Kim, " Bose – Einstein Condensate Theory of Deuteron Fusion in Metal " Purdue University, 2010.

29. Bulent Y. , Sakir A. , et al, " Stochastic Semi – Classical Description of Sub – Barrier Fusion Reactions ", EDP Sciences, 2011.

30. J.K. Bitok, F.G. Kanyeki, et al, " Calculation of Fusion Reaction Cross Section and Angular Momentum Windo $^{6}Li, ^{16}O , ^{56}FE , ^{86}KR$ on Fusion Reaction with ^{208}pb at $E_{lab} = 500\ MeV$ " International Journal of Physics and Mathematical Sciences, Vol. 2, 2012.

31. E.N. Tsyganov, S.B. Dabagov, et al in, " Cold Fusion Continues ", North Caucasus State Technical University, Stuvropol, 2012.

32. Rajdeep S., Andreas M. , et al, " Tunneling Through Coulombic Barriers : Quantum Control of Nuclear Fusion ", Yale University, Vol. 110, 2012.

33. Leo G. Sapogin, Yu. A. Ryabov, " Low Energy Nuclear Reactions [LENR] – and Nuclear Transmutations at Unitary Quantum Theory ", " International Journal of Physics and Astronomy, Vol. 1, No. 1, December, 2013.

34. Igor D. Kaganovich, Ronald C. Davidson, et al, " Comparison of Quantum Mechanical and Classical Trajectory Calculations of Cross Section for Ion – Atom Impact Ionization of Negative –and Positive – ions for Heavy Ion Fusion Application ", Prenceton University, December, 2013.

35. Falah K. Ahmed, Fouad A. Majeed, et al, " The Effect of Break up on The Total Fusion Reaction Cross Section of Stable Weakly Bound Nuclei ", University of Babylon, 2013.

36. P. Eudes1, Z. Basrak2, et al, " Towards A unified Description of Fusion Evaporation – Residue Cross Sections Above The Barrier ", Europhysics Letters, 2013.

37. V. Yu. Denisov, " Nucleus – Potential with Shell – Correction Contribution and Deep Sub – Barrier Fusion of Heavy Nuclei ", National University of Kiev Prospect Glushkova 2, April, 2014.

38. Decrton M. , Massaut V. , Inge Uytdenhouwen, Johan Braet, et al, "Controlled nuclear fusion:The energy of the stars on earth" , Open Report SCK.CEN- BLG -1049, 2007.

39. L.M., " Hively Nuclei Fusion ", 17,837, 1977.

40. Bosch, H.S. , Hale, G.M. , " Nuclei Fusion " 32, 1992.

41. Book, " NRL Plasma Formulary ", publ. 6790-02-450, Rev. Naval Research Laboratory, Washington, December, 2002.

42. R.R. Peterson, J.J. Macfarlane , and G.A. Moses, " BUCKY-A1-D radiation Hydrodynamics Code for Simulation Inertial Confinement fusion High Energy Density Plasma ", UWFDM-984, University of Wisconsin , August, 1995.
43. P.B. Radha , V.N. Goncharvo, T.G.B. et al, " Two Dimension Simulations Of Plastic Shell Direct – Drive Implosions on OMEGA", (to appear in Physics Plasma).
44. T.A. Heltemes, G.A. Moses, et al, "Analysis of an Improved Fusion Reaction Rate Model for Use in Fusion Plasma Simulation", University of Wisconsin Madison, WI53706, April, 2005.

45. G. Gamow , "Nuclear Energy Sources and Stellar Evolution," *Phys. Rev.* **53**, 595 (1938).

46. G. Gamow , "Zur Quantentheorie des Atomkernes," *Zeits. f. Physik*. **51**, 204 (1928).

47. X. Z. Li, "Overcoming of the Gamow Tunneling Insufficiencies by Maximizing a Damp-Matching Resonant Tunneling," *Czechoslovak Journal of Physics*, **49**, 985 (1999).

48. X. Z. Li, C. X. Li and H. F. Huang, "Maximum Value of the Resonant Tunneling Current through the Coulomb Barrier," *Fusion Technology*, **36**, 324 (1999).

49. X. Z. Li, J. Tian , M. Y. Mei and C. X. Li, "Sub-barrier Fusion and Selective Resonant Tunneling," *Phys. Rev.* ,**C 61**, 024610 (2000).

50. H. Feshbach, *Theoretical Nuclear Physics*, John Wiley & Sons, Inc. (New York) 1992, p.488.

51. D. L. Book, *NRL Plasma Formulary*, NRL Publication 177-4405, Naval Research Laboratory, (revised 1990) p.44.

52. B.H.Duane, "Fusion Cross Section Theory," *BWNL-1685* (Pacific North West Laboratory report, 1972) p.76.

53. I.H. Hutchinson ", Principles of Plasma Diagnostics", Second Addition , Cambrigde University Press, 2002.

54. Landau LD, Lifschitz EM (1969) Mechanics. Pergamon Press

55. Gamov G, Critchfield CL (1951) The Theory Atomic Nucleus and Nuclear Energy Sources. Clarendon Press, Ch. X, eq. 2.

56. Landau LD, Lifschitz EM (1987) Quantum Mechanics. 3rd edn., Pergamon Press.

57. Duane BH (1972) Fusion Cross-section Theory. Brookhaven National Laboratory Report BNWL-1685, pp. 75–92.

58. Li ZX, Wie MQ, Liu B (2008) Nucl. Fusion 48, 125003.

59. B.H.Duane, "Fusion Cross Section Theory," *BWNL-1685* (Pacific North West Laboratory report, 1972) p.76

60. Commons-wikiedia.org/wiki/file DT-fusion-reaction-power- density jpg 24, May, 2007.

61. Stefano Atzeni, Jurgen Meyer-Ter-Vehn; , “The physics of Intertial: Beam plasma interaction, Hydrodynamics ,Hot ,Dense matter”, Clarenon press –Oxford,2004.

.1

1. CM M. Keilhacker, A. Gibson, C. Gormezano and P.H. Rebut, “The Scientific Success of JET”, Nuclear Fusion, Volume 41, Number 12, 2001, pp. 1925-1935.

2. JT-60 Team, “Review of JT-60U Experimental Results in 1998”, JAERI 99-048.

3. Jordan E. Merelli, "Plasma position control in the Stor – M Tokamak" P.1 January, 2003 .

4. Engida H. Selato, "Nuclear Fusion Energy" Addis Ababa University, P.3, Julay, 2010.

5. M. Kikuchi, "Hydrogen Fusion: Light Nuclei and Theory of Fusion Reactions" Springer, P.15, 2011.

6. Asimov I (1991) Atom. Nightfall Inc.

7. Atzeni. "Nuclear Fusion Reactions" Chap.1, P.3, 2004.

8. J. M. Blatt, V. F. Weisskopf:" Theoretical Nuclear Physics", Chapter VIII, Springer-Verlag, 1979

9. Akito T. , Norio Y. "Fusion Rates of Bosonized Condensates", Osaka Univercity, Sept. 2006.

10. A. Takahshi, et al: JJAP, 41(2001)pp.7031-7046

11. M. Ohta, A. Takahashi: JJAP, 42(2002)pp.645-649

12. A. Takahashi:" Theoretical backgrounds for transmutation reactions", ppt slides for Sunday School of ICCF10, see http://www.lenr-canr.org/ Special Collection for ICCF10.

13. B. Povh, K. Rith, C. Scholtz, F. Zetsche: Teilchen und Kerne, Springer, 1994.

14. K. Yagi: Nuclear Physics (in Japanese), Asakura, Tokyo, 1971

15. L. I. "Schiff:Quantum Mechanics", McGraw-Hill (1955)

16. P. M. Morse, H. Feshbach; "Methods of Theoretical Physics", McGraw-Hill (1953)

17. X. Z. Li, et al: Phys. Rev. C, 61(2000)24610

18. Xing Z. Li , "Nuclear Physics for Nuclear Fusion ", The Journal of American Society, Vol. 41, No. 63,P1, 2002.

19. Igor D. Kaganovich, Edward A. Startsev, et al, "Scaling Cross Section for Ion – Atom Impact Ionization" Prenceton University, Vol. 11, No. 3,P1, November, 2003.

20. V. I. Zagrebaev* and V. V. Samarin, " Near – Barrier Fusion of Heavy Nuclei : Coupling of Channels", Joint Institute for Nuclear Research, Vol. 67, No. 8,P1, November, 2003.

21. M. Yu. Romanovsky and W. Ebeling, " Fluctuations of Electric Microfields in Laser – Produced Ion Clusters : Enhancement of Nuclear Fusion", Humboldt University Berlen, Vol. 14, No. 6,P1, June, 2003.

22. Xing Z. Li, Bin l., et al, " Fusion Cross Section for Inertial Fusion Energy ", Cambridge University Press,P1, July, 2004.

23. L.F. Canto, R. Donangelo, et al, " Semiclassical Treatment of Fusion Processes in Collision of Weakly Bound Nuclei ", Institute de Fisica,P1, 2005.

24. L.F. Canto, R. Donangelo, et al, " Theory of Breakup and Fusion of Weakly Bound Nuclei ", Institute de Fisica,P1, 2005.

25. Ruggero M. Santilli, " Controlled Intermediate Nuclear ", Institute for Basic Research ",P1, 2008.

26. Mark D., " Inertial Electrostatic Confinement Fusion Provides A potential Break Through in Designing and Implementing Practical Fusion Power Plants ", www.askamr.com ,P1, 2008.

27. Xing Z. Li, Qing M. Wei ,et al, " A new Simple Formula for Fusion Cross Section Light Nuclei ", Tsinghua University,P1, October, 2008.

28. Yeong E. Kim, " Bose – Einstein Condensate Theory of Deuteron Fusion in Metal " Purdue University,P1, 2010.

29. Bulent Y. , Sakir A. , et al, " Stochastic Semi – Classical Description of Sub – Barrier Fusion Reactions ", EDP Sciences,P1, 2011.

30. J.K. Bitok, F.G. Kanyeki, et al, " Calculation of Fusion Reaction Cross Section and Angular Momentum Windo ^{6}Li, ^{16}O , ^{56}FE , ^{86}KR on Fusion Reaction with ^{208}pb at $E_{lab} = 500\ MeV$ " International Journal of Physics and Mathematical Sciences, Vol. 2,P1, 2012.

31. E.N. Tsyganov, S.B. Dabagov, et al in, " Cold Fusion Continues ", North Caucasus State Technical University, Stuvropol,P1, 2012.

32. Rajdeep S., Andreas M. , et al, " Tunneling Through Coulombic Barriers : Quantum Control of Nuclear Fusion ", Yale University, Vol. 110,P1, 2012.

33. Leo G. Sapogin, Yu. A. Ryabov, " Low Energy Nuclear Reactions [LENR] – and Nuclear Transmutations at Unitary Quantum Theory ", " International Journal of Physics and Astronomy, Vol. 1, No. 1,P1, December, 2013.

34. Igor D. Kaganovich, Ronald C. Davidson, et al, " Comparison of Quantum Mechanical and Classical Trajectory Calculations of Cross Section for Ion – Atom Impact Ionization of Negative –and Positive – ions for Heavy Ion Fusion Application ", Prenceton University,P1, December, 2013.

35. Falah K. Ahmed, Fouad A. Majeed, et al, " The Effect of Break up on The Total Fusion Reaction Cross Section of Stable Weakly Bound Nuclei ", University of Babylon,P1, 2013.

36. P. Eudes1, Z. Basrak2, et al, " Towards A unified Description of Fusion Evaporation – Residue Cross Sections Above The Barrier ", Europhysics Letters,P1, 2013.

37. V. Yu. Denisov, " Nucleus – Potential with Shell – Correction Contribution and Deep Sub – Barrier Fusion of Heavy Nuclei ", National University of Kiev Prospect Glushkova 2, April, 2014.

38. Decrton M. , Massaut V. , Inge Uytdenhouwen, Johan Braet, et al, "Controlled nuclear fusion:The energy of the stars on earth" , Open Report SCK.CEN- BLG -1049, 2007.

39. L.M., " Hively Nuclei Fusion ", 17,837, 1977.

40. Bosch, H.S. , Hale, G.M. , " Nuclei Fusion " 32, 1992.

41." NRL Plasma Formulary ", publ. 6790-02-450, Rev. Book, Naval Research Laboratory, Washington, December, 2002.

`

42. R.R. Peterson, J.J. Macfarlane , and G.A. Moses, " BUCKY-A1-D radiation Hydrodynamics Code for Simulation Inertial Confinement fusion High Energy Density Plasma ", UWFDM-984, University of Wisconsin , August, 1995.
43. P.B. Radha , V.N. Goncharvo, T.G.B. et al, " Two Dimension Simulations Of Plastic Shell Direct – Drive Implosions on OMEGA", (to appear in Physics Plasma).
44. T.A. Heltemes, G.A. Moses, et al, "Analysis of an Improved Fusion Reaction Rate Model for Use in Fusion Plasma Simulation", University of Wisconsin Madison, WI53706, April, 2005.

45. G. Gamow , "Nuclear Energy Sources and Stellar Evolution," *Phys. Rev.* **53**, 595 (1938).

46. G. Gamow , "Zur Quantentheorie des Atomkernes," *Zeits. f. Physik*. **51**, 204 (1928).

47. X. Z. Li, "Overcoming of the Gamow Tunneling Insufficiencies by Maximizing a Damp-Matching Resonant Tunneling," *Czechoslovak Journal of Physics*, **49**, 985 (1999).

48. X. Z. Li, C. X. Li and H. F. Huang, "Maximum Value of the Resonant Tunneling Current through the Coulomb Barrier," *Fusion Technology*, **36**, 324 (1999).

49. X. Z. Li, J. Tian , M. Y. Mei and C. X. Li, "Sub-barrier Fusion and Selective Resonant Tunneling," *Phys. Rev.* ,**C 61**, 024610 (2000).

50. H. Feshbach, *Theoretical Nuclear Physics*, John Wiley & Sons, Inc. (New York) 1992, p.488.

51. D. L. Book, *NRL Plasma Formulary*, NRL Publication 177-4405, Naval Research Laboratory, (revised 1990) p.44.

52. B.H.Duane, "Fusion Cross Section Theory," *BWNL-1685* (Pacific North West Laboratory report, 1972) p.76.

53. I.H. Hutchinson ", Principles of Plasma Diagnostics", Second Addition , Cambrigde University Press, 2002.

54. Landau LD, Lifschitz EM Mechanics. Pergamon Press, (1969).

55. Gamov G, Critchfield CL The Theory Atomic Nucleus and Nuclear Energy Sources. Clarendon Press, Ch. X, eq. 2, (1951).

56. Landau LD, Lifschitz EM Quantum Mechanics. 3rd edn., Pergamon Press, (1987).

57. Duane BH Fusion Cross-section Theory. Brookhaven National Laboratory Report BNWL-1685, pp. 75–92, (1972)

58. Li ZX, Wie MQ, Liu B (2008) Nucl. Fusion 48, 125003.

59. B.H.Duane, "Fusion Cross Section Theory," *BWNL-1685* (Pacific North West Laboratory report, 1972) p.76

60. Commons-wikiedia.org/wiki/file, DT-fusion-reaction-power-density, jpg 24, May, 2007.

61. Stefano Atzeni, Jurgen Meyer-Ter-Vehn; , “The physics of Intertial: Beam plasma interaction, Hydrodynamics ,Hot ,Dense matter”, Clarenon press –Oxford,2004.

.1